CHAPTER

ELEVEN

INTERNAL TRANSPORT PROCESSES— REACTION AND DIFFUSION IN POROUS CATALYSTS

Essentially all of the active surface of porous catalyst pellets is internal (see p. 327). The reaction that occurs within the pellet consumes reactant and evolves (or absorbs) the heat of reaction. This, in turn, induces *internal* concentration and temperature gradients which can be large enough to cause a significant variation in rate of reaction with position inside the pellet.

At steady state the average rate for the whole pellet will be equal to the global rate at the location of the pellet in the reactor. The concentration and temperature of the bulk fluid at this location may not be equal to the values at the outer surface of the pellet. In Chap. 10 we studied how to account for these *external* transport resistances, but we did not consider the influence of the internal concentration and temperature gradients. This latter effect is the objective of the present chapter. That is to say, we want to evaluate the *average* rate for the whole pellet in terms of the concentration and temperature at the outer surface. Then the results of Chaps. 10 and 11 can be combined to express the rate in terms of the known bulk properties for use in design.

Because there is a continuous variation in concentration and temperature with radius of the pellet, *differential* conservation equations are required to describe the concentration and temperature profiles. These profiles are used with the intrinsic rate equation to integrate through the pellet and so obtain the average rate for the pellet. The differential equations involve the effective† diffusivity

† In the remainder of the text the term "effective" is used to indicate that a transport coefficient applies to a porous material, as distinguished from a homogeneous region. Effective diffusivities D_e and thermal conductivities k_e are based on a unit of *total area* (void plus nonvoid) perpendicular to the direction of transport. For example, for diffusion in a spherical catalyst pellet at radius r, D_e is based on the area $4\pi r^2$.

and thermal conductivity of the porous pellet. Data and theories for these quantities are given in Secs. 11-4 to 11-6, and in Secs. 11-7 to 11-11 the results are used to establish the rate for the whole pellet. The method of combining the effects of *internal* and *external* transport resistance to give the global rate in terms of bulk fluid properties is discussed in Example 11-8 and also in Chap. 12.

The effect of intrapellet mass transfer is to reduce the reactant concentration within the pellet. Hence, the average rate will be less than what it would be if there were no internal concentration gradient. The effect of the temperature gradient is to increase the rate for an exothermic reaction, the opposite of the mass transfer effect. This is because intrapellet temperatures will be greater than surface values. For endothermic reactions temperature and concentration gradients both reduce the rate below that evaluated at outer-surface conditions.

For a gaseous reaction accompanied by a change in number of moles, an intrapellet gradient in total pressure will also develop (at steady state). If the moles decrease, there will be a flow of reactant toward the center of the pellet due to this total-pressure gradient. This augments the diffusion of reactant inward toward the center of the pellet and retards the diffusion of product outward. Unless the decrease in number of moles is very large, which is unlikely, the effect on the average rate is small.† Also, it should be remembered that all intrapellet-transport effects will become less important as the pellet size decreases. For fluidized-bed and slurry reactors intraparticle transport processes can usually be neglected.

INTRAPELLET MASS TRANSFER

It is seldom possible to predict diffusion rates in porous materials by simply correcting bulk-phase diffusivities for the reduction in cross-sectional area due to the solid phase. There are several reasons for this:

1. The tortuous, random, and interconnected arrangement of the porous regions makes the length of the diffusion path unknown.
2. The diffusion in the pore volume itself will be influenced by the pore walls, provided the diffusing molecule is likely to collide with a wall rather than another molecule. This often is the case for gaseous systems. Then the pore-volume contribution to total mass transport is not dependent solely on the *bulk diffusivity*, but may be affected (or determined) by the *Knudsen diffusivity*.
3. A catalyst is characterized as a substance which adsorbs reactant. When it is adsorbed it may be transported either by desorption into the pore space or by migration to an adjacent site on the surface. The contribution of surface diffusion probably is small in most cases, but it must be added to the diffusion in the pore volume to obtain the total mass transport.

† See A. Wheeler in P. H. Emmett (ed.), "Catalysis," vol. II, p. 143, Reinhold Publishing Corporation, New York, 1955; Von E. Wicke and Peter Hugo, *Z. Phys. Chem.*, **28**, 26 (1961); S. Otani, N. Wakao, and J. M. Smith, *AIChE J.*, **10**, 135 (1965); N. Wakao, S. Otani, and J. M. Smith, *AIChE J.*, **11**, 435 (1965).

Surface diffusion is not well understood, and rates of diffusion by this mechanism cannot yet be predicted. We must be content with summarizing in Sec. 11-4 the available data for surface migration. Volume diffusion in a straight cylindrical pore is amenable to analysis. Hence the procedure used (see Sec. 11-3) to predict an effective diffusivity is to combine the established equations for diffusion in a single cylindrical pore with a geometric model of the pore structure of the catalyst pellet. If the surface diffusivity is known for the surface of a cylindrical pore, it can be used with the same model to obtain the total mass-transport rate (in the absence of flow due to a total-pressure gradient). The nature of gaseous diffusion in cylindrical pores is discussed in Sec. 11-1. When the reaction mixture in the pore is liquid Knudsen diffusion does not occur, but uncertainty as to how the bulk diffusivity varies with concentration is a complicating feature. The effective length of the diffusion path is determined by the pore structure of the pellet. Hence the path length is intimately connected with the model chosen to represent the porous catalyst. Such models are considered in Sec. 11-3.

It is evident from the foregoing discussion that the effective diffusivity cannot be predicted accurately for use under reaction conditions unless surface diffusion is negligible and a valid model for the pore structure is available. The prediction of an effective thermal conductivity is also difficult. Hence sizable errors are frequent in predicting the global rate from the rate equation for the chemical step on the interior catalyst surface. This is not to imply that for certain special cases accuracy is not possible (see Sec. 11-9). It does mean that heavy reliance must be placed on experimental measurements for effective diffusivities and thermal conductivities. Also note from some of the examples and data mentioned later that intrapellet resistances can greatly affect the rate. Hence the problem is significant.

Only a brief account will be given of the considerable theory on *special* aspects of isothermal mass transfer. More emphasis will be placed on interpretation of laboratory-reactor data with respect to the importance of intrapellet resistances.

11-1 Gaseous Diffusion in Single Cylindrical Pores

Basic Equations For many catalysts and reaction conditions (especially pressure) both bulk and Knudsen diffusion contribute to the mass-transport rate within the pore volume. For some years the proper combination of the two mechanisms was in doubt. About 1961 three independent investigations† proposed identical equations for the rate of diffusion (in a binary gaseous mixture of A and B) in terms of the bulk diffusivity $\mathscr{D}_{AB}$ and Knudsen diffusivity $\mathscr{D}_K$. If N_A is the molal flux of A, it is convenient to represent the result as

$$N_A = -\frac{p_t}{R_g T} D \frac{dy_A}{dx} \tag{11-1}$$

† R. B. Evans, III, G. M. Watson, and E. A. Mason, *J. Chem. Phys.*, 35, 2076 (1961); L. B. Rothfeld, *AIChE J.*, 9, 19 (1963); D. S. Scott and F. A. L. Dullien, *AIChE J.*, 8, 29 (1962).

where y_A is the mole fraction of A, x is the coordinate in the direction of diffusion, and D is a *combined* diffusivity given by

$$D = \frac{1}{(1 - \alpha y_A)/\mathscr{D}_{AB} + 1/(\mathscr{D}_K)_A} \tag{11-2}$$

The quantity α is related to the ratio of the diffusion rates of A and B by

$$\alpha = 1 + \frac{N_B}{N_A} \tag{11-3}$$

For reactions at steady state, α is determined by the stoichiometry of the reaction. For example, for the reaction $A \rightarrow B$, reaction and diffusion in a pore would require equimolal counterdiffusion; that is, $N_B = -N_A$. Then $\alpha = 0$, and the effective diffusivity is

$$D = \frac{1}{1/\mathscr{D}_{AB} + 1/(\mathscr{D}_K)_A} \tag{11-4}$$

When the pore radius is large, Eqs. (11-1) and (11-2) reduce to the conventional constant-pressure form for bulk diffusion. For this condition $(\mathscr{D}_K)_A \rightarrow \infty$. Then combining Eqs. (11-1) to (11-3) gives

$$N_A = -\frac{p_t}{R_g T}\mathscr{D}_{AB}\frac{dy_A}{dx} + y_A(N_A + N_B) \tag{11-5}$$

If, in addition, the diffusion is equimolal, $N_B = -N_A$. Eq. (11-5) may be written

$$N_A = \frac{-p_t}{R_g T}\mathscr{D}_{AB}\frac{dy_A}{dx} \tag{11-6}$$

If the pore radius is very small, collisions will occur primarily between gas molecules and pore wall, rather than between molecules. Then the Knudsen diffusivity becomes very low, and Eqs. (11-1) and (11-2) reduce to

$$N_A = -\frac{p_t}{R_g T}(\mathscr{D}_K)_A\frac{dy_A}{dx} \tag{11-7}$$

This equation is the usual one† expressing Knudsen diffusion in a long capillary.

Although Eq. (11-2) is the proper one to use for regions where both Knudsen and bulk diffusion are important, it has a serious disadvantage: the combined diffusivity D is a function of gas composition y_A in the pore. This dependency on composition carries over to the effective diffusivity in porous catalysts (see Sec. 11-3) and makes it difficult later to integrate the combined diffusion and transport equations. The variation of D with y_A is usually not strong (see Example 11-3). Therefore it has been almost universal,‡ in assessing the importance of

† M. Knudsen, *Ann. Physik*, **28**, 75 (1909); N. Wakao, S. Otani, and J. M. Smith, *AIChE J.*, **11**, 435 (1965).

‡ N. Wakao and J. M. Smith [*Ind. Eng. Chem., Fund. Quart.*, 3, 123 (1964)] used the general equations (11-1) and (11-2) in developing expressions for intrapellet effects for isothermal first-order reactions.

intrapellet resistances, to use a composition-independent form for D, for example, Eq. (11-4). In fact, the concept of a single effective diffusivity loses its value if the composition dependency must be retained. Note also that the problem disappears when the reaction stoichiometry is such that diffusion is countercurrent and equimolal.

Effective diffusivities in porous catalysts are usually measured under conditions where the *pressure is maintained constant by external means* (experimental methods are described in Sec. 11-3). Under this condition, and for a binary counterdiffusing system, the ratio N_B/N_A is the same regardless of the extent of Knudsen and bulk diffusion. Evans et al† have shown this constant ratio to be (at constant pressure)

$$\frac{N_B}{N_A} = -\sqrt{\frac{M_A}{M_B}} \tag{11-8}$$

or

$$\alpha = 1 - \sqrt{\frac{M_A}{M_B}}$$

where M represents the molecular weight. Equation (11-8) applies for nonreacting conditions. When reaction occurs, stoichiometry determines α (see Example 11-3).

Calculation of Diffusivities In analyzing Knudsen and bulk diffusivities the important parameter is the size of the pore with respect to the mean free path. The bulk diffusivity is a function of the molecular velocity and the mean free path; that is, it is a function of temperature and pressure. The Knudsen diffusivity depends on the molecular velocity v and the pore radius a. In terms of simple kinetic theory, these two diffusivities may be described by the equations

$$\mathscr{D}_{AB} = \tfrac{1}{3}\bar{v}\lambda \qquad \left(\lambda \sim \frac{1}{p}\right) \tag{11-9}$$

$$(\mathscr{D}_K)_A = \tfrac{2}{3}a\bar{v} \tag{11-10}$$

where λ is the mean free path. Since λ is of the order of 1000 Å for gases at atmospheric pressure, diffusion in micropores of a catalyst pellet will be predominantly by the Knudsen mechanism. This would be the case for a material such

† R. B. Evans, III, G. M. Watson, and E. A. Mason, *J. Chem. Phys.*, 35, 2076 (1961).

---

† Values of σ and ε/k_B are from J. O. Hirschfelder, C. F. Curtiss, and R. B. Bird, "Molecular Theory of Gases and Liquids," pp. 1110-1112, John Wiley & Sons, Inc., New York, 1954 (also Addenda and Corrigenda, p. 11). The above values are computed from viscosity data and are applicable for temperatures above 100 K.

‡ Values of T_c, p_c, and V_c are from K. A. Kobe and R. E. Lynn, Jr., *Chem. Rev.*, **52**, 117-236 (1952); F. D. Rosinni (ed.), *Am. Petrol. Inst. Res. Proj.*, Carnegie Institute of Technology, **44** (1952).

Source: By permission from R. B. Bird, W. E. Stewart, and E. N. Lightfoot, "Transport Phenomena," John Wiley & Sons, Inc., New York, 1960.

Table 11-1 Lennard-Jones constants and critical properties

Substance	Molecular weight	Lennard-Jones parameters† σ, Å	ε/k_B, K	Critical constants‡ T_c, K	p_c, atm	V_c, cm³/g mole
Light elements						
H_2	2.016	2.915	38.0	33.3	12.80	65.0
He	4.003	2.576	10.2	5.26	2.26	57.8
Noble gases						
Ne	20.183	2.789	35.7	44.5	26.9	41.7
Ar	39.944	3.418	124.0	151.0	48.0	75.2
Kr	83.80	3.61	190.0	209.4	54.3	92.2
Xe	131.3	4.055	229.0	289.8	58.0	118.8
Simple polyatomic substances						
Air	28.97	3.617	97.0	132.0	36.4	86.6
N_2	28.02	3.681	91.5	126.2	33.5	90.1
O_2	32.00	3.433	113.0	154.4	49.7	74.4
O_3	48.00	.....	.....	268.0	67.0	89.4
CO	28.01	3.590	110.0	133.0	34.5	93.1
CO_2	44.01	3.996	190.0	304.2	72.9	94.0
NO	30.01	3.470	119.0	180.0	64.0	57.0
N_2O	44.02	3.879	220.0	309.7	71.7	96.3
SO_2	64.07	4.290	252.0	430.7	77.8	122.0
F_2	38.00	3.653	112.0			
Cl_2	70.91	4.115	357.0	417.0	76.1	124.0
Br_2	159.83	4.268	520.0	584.0	102.0	144.0
I_2	253.82	4.982	550.0	800.0		
Hydrocarbons						
CH_4	16.04	3.822	137.0	190.7	45.8	99.3
C_2H_2	26.04	4.221	185.0	309.5	61.6	113.0
C_2H_4	28.05	4.232	205.0	282.4	50.0	124.0
C_2H_6	30.07	4.418	230.0	305.4	48.2	148.0
C_3H_6	42.08	.....	.....	365.0	45.5	181.0
C_3H_8	44.09	5.061	254.0	370.0	42.0	200.0
n-C_4H_{10}	58.12	.....	.....	425.2	37.5	255.0
i-C_4H_{10}	58.12	5.341	313.0	408.1	36.0	263.0
n-C_5H_{12}	72.15	5.769	345.0	469.8	33.3	311.0
n-C_6H_{14}	86.17	5.909	413.0	507.9	29.9	368.0
n-C_7H_{16}	100.20	.....	.....	540.2	27.0	426.0
n-C_8H_{18}	114.22	7.451	320.0	569.4	24.6	485.0
n-C_9H_{20}	128.25	.....	.....	595.0	22.5	543.0
Cyclohexane	84.16	6.093	324.0	553.0	40.0	308.0
C_6H_6	78.11	5.270	440.0	562.6	48.6	260.0
Other organic compounds						
CH_4	16.04	3.822	137.0	190.7	45.8	99.3
CH_3Cl	50.49	3.375	855.0	416.3	65.9	143.0
CH_2Cl_2	84.94	4.759	406.0	510.0	60.0	
$CHCl_3$	119.39	5.430	327.0	536.6	54.0	240.0
CCl_4	153.84	5.881	327.0	445.4	45.0	276.0
C_2N_2	52.04	4.38	339.0	400.0	59.0	
COS	60.08	4.13	335.0	378.0	61.0	
CS_2	76.14	4.438	488.0	552.0	78.0	170.0

as silica gel, where the mean pore radius is from 15 to 100 Å (see Table 8-1). For a pelleted catalyst of alumina with the pore-volume distribution shown in Fig. 8-8, the mean macropore radius is about 8000 Å. At atmospheric pressure bulk diffusion would prevail in these pores. In the micropores of the same pellet, where $\bar{a} = 20$ Å, diffusion would be by the Knudsen process. Since the mean free path is inversely proportional to pressure, bulk diffusivity becomes more important as the pressure increases.

For more accurate calculations the *Chapman-Enskog formula*† has been found suitable for evaluating the bulk diffusivity at moderate temperatures and pressures. The equation is (for the binary gas mixture A, B)

$$\mathscr{D}_{AB} = 0.0018583 \frac{T^{3/2}(1/M_A + 1/M_B)^{1/2}}{p_t \sigma_{AB}^2 \Omega_{AB}} \tag{11-11}$$

where $\mathscr{D}_{AB}$ = bulk diffusivity, cm^2/s
T = temperature, K
M_A, M_B = molecular weights of gases A and B
p_t = total pressure of the gas mixture, atm
σ_{AB}, ε_{AB} = constants in the Lennard-Jones potential-energy function for the molecular pair AB; σ_{AB} is in Å.
Ω_{AB} = collision integral, which would be unity if the molecules were rigid spheres and is a function of $k_B T/\varepsilon_{AB}$ for real gases (k_B = Boltzmann's constant)

Since the Lennard-Jones potential-energy function is used, the equation is strictly valid only for nonpolar gases. The Lennard-Jones constants for the unlike molecular pair AB can be estimated from the constants for like pairs AA and BB:

$$\sigma_{AB} = \tfrac{1}{2}(\sigma_A + \sigma_B) \tag{11-12}$$

$$\varepsilon_{AB} = (\varepsilon_A \varepsilon_B)^{1/2} \tag{11-13}$$

The force constants for many gases are given in the literature and are summarized in Table 11-1. Those that are not available otherwise may be approximated by the expressions

$$\sigma = 1.18\, V_b^{1/3} \tag{11-14}$$

$$\frac{k_B T}{\varepsilon} = 1.30 \frac{T}{T_c} \tag{11-15}$$

where k_B = Boltzmann's constant
T_c = critical temperature
V_b = volume per mole (cm^3/g mole) at normal boiling point

If necessary, V_b may be estimated by adding the increments of volume for the atoms making up the molecule (Kopp's law). Such increments are given in Table

† See J. O. Hirschfelder, C. F. Curtiss, and R. B. Bird, "Molecular Theory of Gases and Liquids," pp. 539, 578, John Wiley & Sons, Inc., New York, 1954.

Table 11-2 Volume increments for estimating molecular volume at normal boiling point

Kind of atom in molecule	Volume increment, cm^3 g mol
Carbon	14.8
Chlorine, terminal as R—Cl	21.6
Chlorine, medial as —CHCl—	24.6
Fluorine	8.7
Helium	1.0
Hydrogen	3.7
Mercury	15.7
Nitrogen in primary amines	10.5
Nitrogen in secondary amines	12.0
Oxygen in ketones and aldehydes	7.4
Oxygen in methyl esters and ethers	9.1
Oxygen in ethyl esters and ethers	9.9
Oxygen in higher esters and ethers	11.0
Oxygen in acids	12.0
Oxygen bonded to S, P, or N	8.3
Phosphorus	27.0
Sulfur	25.6
For organic cyclic compounds	
3-membered ring	−6.0
4-membered ring	−8.5
5-membered ring	−11.5
6-membered ring	−15.0
Naphthalene	−30.0
Anthracene	−47.5

Source: In part from C. N. Satterfield and T. K. Sherwood, "The Role of Diffusion in Catalysis," p. 9, Addison-Wesley Publishing Company, Reading, Mass., 1963.

11-2. The collision integral Ω_{AB} is given as a function of $k_B T/\varepsilon_{AB}$ in Table 11-3. From these data and the equations, binary diffusivities may be estimated for any gas. For polar gases, or for pressures above 0.5 critical pressure, the errors may be greater than 10%. The effects of composition on $\mathcal{D}$ are small for gases at moderate conditions, so that the same procedure may be used as an approximation for multicomponent mixtures. An improved result for mixtures may be obtained from empirical correlations.†

For evaluating the Knudsen diffusivity we may use the following equation for the average molecular velocity $\bar{v}$ for a component of gas in a mixture:

$$\bar{v}_A = \left(\frac{8R_g T}{\pi M_A}\right)^{1/2} \tag{11-16}$$

† See R. C. Reid, J. M. Prausnitz, and T. K. Sherwood, "The Properties of Gases and Liquids", 3d ed., chap. 11, McGraw-Hill Book Company, New York, 1977.

Table 11-3 Values of Ω_{AB} for diffusivity calculations (Lennard-Jones model)

$k_B T/\varepsilon_{AB}$	Ω_{AB}	$k_B T/\varepsilon_{AB}$	Ω_{AB}
0.30	2.662	2.0	1.075
0.35	2.476	2.5	1.000
0.40	2.318	3.0	0.949
0.45	2.184	3.5	0.912
0.50	2.066	4.0	0.884
0.55	1.966	5.0	0.842
0.60	1.877	7.0	0.790
0.65	1.798	10.0	0.742
0.70	1.729	20.0	0.664
0.75	1.667	30.0	0.623
0.80	1.612	40.0	0.596
0.85	1.562	50.0	0.576
0.90	1.517	60.0	0.560
0.95	1.476	70.0	0.546
1.00	1.439	80.0	0.535
1.10	1.375	90.0	0.526
1.20	1.320	100.0	0.513
1.30	1.273	200.0	0.464
1.40	1.233	300.0	0.436
1.50	1.198	400.0	0.417
1.75	1.128		

Source: By permission from J. O. Hirshfelder, C. F. Curtiss, and R. B. Bird, "Molecular Theory of Gases and Liquids," pp. 1126, 1127, John Wiley & Sons, Inc., New York, 1954.

Combining this with Eq. (11-10) gives a working expression for $(\mathscr{D}_K)_A$ in a circular pore of radius a,

$$(\mathscr{D}_K)_A = 9.70 \times 10^3 a \left(\frac{T}{M_A}\right)^{1/2} \tag{11-17}$$

where $(\mathscr{D}_K)_A$ is in square centimeters per second, a is in centimeters, and T is in degrees Kelvin.

Example 11-1 Estimate the diffusivity of SO_2 for the conditions of Example 10-1.

SOLUTION The gas composition is about 94% air, with the remainder SO_2 and SO_3. Hence a satisfactory simplification is to consider the system as a binary mixture of air and SO_2.

From Table 11-1, for air

$$\frac{\varepsilon}{k_B} = 97°\text{K} \qquad \sigma = 3.617\ \text{Å or } 3.617 \times 10^{-10}\ \text{m, or } 0.3617\ \text{nanometers}$$

and for SO_2

$$\frac{\varepsilon}{k_B} = 252°\text{K} \qquad \sigma = 4.290 \text{ Å } (0.429 \text{ nm})$$

From Eqs. (11-12) and (11-13),

$$\sigma_{AB} = \tfrac{1}{2}(3.617 + 4.290) = 3.953 \text{ Å } (0.3953 \text{ nm})$$

$$\varepsilon_{AB} = k_B[97(252)]^{1/2}$$

At the temperature of 480°C,

$$\frac{k_B T}{\varepsilon_{AB}} = \frac{k_B(753)}{k_B[97(252)]^{1/2}} = 4.8$$

and so, from Table 11-3,

$$\Omega_{AB} = 0.85$$

Substituting all these values in Eq. (11-11) gives

$$\mathscr{D}_{SO_2\text{-air}} = 0.0018583 \frac{753^{3/2}(1/64.1 + 1/28.9)^{1/2}}{(790/760)(3.953)^2(0.85)}$$

$$= 0.629 \text{ cm}^2/\text{s } (0.629 \times 10^{-4} \text{ m}^2/\text{s})$$

Example 11-2 A nickel catalyst for the hydrogenation of ethylene has a mean pore radius of 50 Å. Calculate the bulk and Knudsen diffusivities of hydrogen for this catalyst at 100°C, and 1 and 10 atm pressures, in a hydrogen-ethane mixture.

SOLUTION From Table 11-1, for H_2

$$\frac{\varepsilon}{k_B} = 38 \text{ K} \qquad \sigma = 2.915 \text{ Å}$$

and for C_2H_6

$$\frac{\varepsilon}{k_B} = 230 \text{ K} \qquad \sigma = 4.418 \text{ Å}$$

Then for the mixture, from Eqs. (11-12) and (11-13),

$$\sigma_{AB} = \tfrac{1}{2}(2.915 + 4.418) = 3.67 \text{ Å}$$

$$\varepsilon_{AB} = k_B[38(230)]^{1/2}$$

and

$$\frac{k_B T}{\varepsilon_{AB}} = \frac{273 + 100}{[38(230)]^{1/2}} = 4.00$$

From Table 11-3,

$$\Omega_{AB} = 0.884$$

Substituting these values in the Chapman-Enskog equation (11-11) gives the bulk diffusivity,

$$\mathscr{D}_{H_2,\,C_2H_6} = 0.001858\,\frac{373^{3/2}(1/2.016 + 1/30.05)^{1/2}}{p_t(3.67)^2(0.884)} = \frac{0.86}{p_t}$$

This gives 0.86 cm²/s at 1 atm, or 0.086 cm²/s at 10 atm.

The Knudsen diffusivity, which is independent of pressure, is obtained from Eq. (11-17) as

$$(\mathscr{D}_K)_{H_2} = 9.70 \times 10^3(50 \times 10^{-8})\left(\frac{373}{2.016}\right)^{1/2} = 0.065 \text{ cm}^2/\text{s}$$

These results show that 1 atm pressure the Knudsen diffusivity is much less than the bulk value. Hence Knudsen diffusion controls the diffusion rate. At 10 atm both bulk and Knudsen diffusivities are important.

Example 11-3 (*a*) Calculate the combined diffusivity of hydrogen in a mixture of ethane, ethylene, and hydrogen in a pore of radius 50 Å (5.0 nm) at two total pressures, corresponding to 1 and 10 atm. Suppose that the pore is closed at one end, and that the open end is exposed to a mixture of ethylene and hydrogen. The pore wall is a catalyst for the reaction

$$C_2H_4 + H_2 \rightarrow C_2H_6$$

The temperature is 100°C.

(*b*) For comparison calculate the combined diffusivity of hydrogen for diffusion through a noncatalytic capillary of radius 50 Å (5.0 nm). Hydrogen is supplied at one end and ethane at the other. The pressure is maintained the same at both ends of the capillary. Make the calculations for two compositions, $y_{H_2} = 0.5$ and 0.8.

SOLUTION (*a*) Assume that the binary H_2—C_2H_6 will be satisfactory for representing the diffusion of hydrogen in the three-component system. From the reaction stoichiometry, the molal diffusion rates of H_2 and C_2H_6 will be equal and in opposite directions. Hence $\alpha = 0$, and Eq. (11-4) is applicable. From the results of Example 11-2,

$$D = \begin{cases} \dfrac{1}{1/0.86 + 1/0.065} = 0.060 \text{ cm}^2/\text{s}\ (0.060 \times 10^{-4}\ \text{m}^2/\text{s}) & \text{at 1 atm} \\ \dfrac{1}{1/0.086 + 1/0.065} = 0.037 \text{ cm}^2/\text{s}\ (0.037 \times 10^{-4}\ \text{m}^2/\text{s}) & \text{at 10 atm} \end{cases}$$

(*b*) For constant-pressure diffusion Eq. (11-2) should be used. From Eq. (11-3)

$$\alpha = 1 + \frac{N_{C_2H_6}}{N_{H_2}} = 1 - \sqrt{\frac{M_{H_2}}{M_{C_2H_6}}} = 1 - \sqrt{\frac{2.016}{30.05}} = 0.741$$

Then at $y_{H_2} = 0.5$, using Eq. (11-2),

$$D = \frac{1}{[1 - 0.741(0.5)]/\mathscr{D}_{H_2-C_2H_6} + 1/(\mathscr{D}_K)_{H_2}} = \frac{1}{0.630/\mathscr{D}_{H_2-C_2H_6} + 1/(\mathscr{D}_K)_{H_2}}$$

For the two pressures this expression gives

$$D = \begin{cases} \dfrac{1}{0.630/0.86 + 1/0.065} = 0.062 \text{ cm}^2/\text{s } (0.062 \times 10^{-4} \text{ m}^2/\text{s}) & \text{at 1 atm} \\ \dfrac{1}{0.630/0.086 + 1/0.065} = 0.044 \text{ cm}^2/\text{s } (0.044 \times 10^{-4} \text{ m}^2/\text{s}) & \text{at 10 atm} \end{cases}$$

At $y_{H_2} = 0.8$ the two results are

$$D = \begin{cases} 0.063 \text{ cm}^2/\text{s } (0.063 \times 10^{-4} \text{ m}^2/\text{s}) & \text{at 1 atm} \\ 0.050 \text{ cm}^2/\text{s } (0.050 \times 10^{-4} \text{ m}^2/\text{s}) & \text{at 10 atm} \end{cases}$$

This example illustrates the following point. The variation of D with y_A depends on the importance of bulk diffusion. At the extreme where the Knudsen mechanism controls, the composition has no effect on D. When bulk diffusion is significant, the effect is a function of α. For equimolal counterdiffusion, $\alpha = 0$ and y_A has no influence on D. In our example, where $\alpha = 0.741$, and at 10 atm pressure, D increased only from 0.044 to 0.050 cm^2/s as y_{H_2} increased from 0.5 to 0.8.

Also note that under reaction conditions in a pore, as in part (*a*), the ratio of the diffusion rates of the species is determined by stoichiometry. In contrast, for nonreacting systems at constant pressure, Eq. (11-8) is applicable.

11-2 Diffusion in Liquids

The mean free path in liquids is so small that Knudsen diffusion is not significant. Thus the diffusion rate is unaffected by the pore diameter and pressure (in the absence of surface diffusion). The *effective* diffusivity is determined by the molecular diffusivity and the pore structure of the catalyst pellet. Since the molecules in liquids are close together, the diffusion of one component is strongly affected by the force fields of nearby molecules and at the pore wall. As a result, diffusivities are concentration dependent and difficult to predict. As an approximation, we may express the diffusion flux of component A in a single cylindrical pore as:

$$N_A = -\mathscr{D}_{AB}\frac{dC_A}{dx} \tag{11-18}$$

where $\mathscr{D}_{AB}$ is the molecular diffusivity of liquid A in a solution of A and B and dC_A/dx is the concentration gradient in the direction of diffusion.

Values of $\mathscr{D}_{AB}$ are much less than those for gases and are, in general, of the order of 1×10^{-5} cm^2/s. For gases (for example, hydrogen) dissolved in liquids

the diffusivity can be an order of magnitude larger, as noted in Examples 10-9 and 11-8. Several correlations are available† for estimating diffusivities in liquids at low concentrations (infinite dilution). These may be used as approximate values in reactor problems but the uncertain and sometimes large effect of concentration on $\mathscr{D}_{AB}$ should not be forgotten.

The major need for liquid-phase diffusivities is in problems involving slurry or trickle-bed reactors. Even though a gas phase is present, the wetting of the catalyst particles by the liquid means that the pores will be essentially filled with liquid. Since diffusivities in liquids are lower than those in gases, internal transport resistances can have a larger effect on the global rate for trickle-bed reactors than for gas-solid (two-phase), fixed-bed reactors. This effect is illustrated in Example 11-8. Even in slurry reactors employing catalyst particles of the order of 100 microns diameter, intraparticle diffusion can affect the global rate.‡

11-3 Diffusion in Porous Catalysts

Considerable experimental data has been accumulated for effective diffusivities in gas-filled pores.§ Since reactors normally are operated at steady state and nearly constant pressure, diffusivities have also been measured under these restraints. The usual apparatus¶ is of the steady-flow type, illustrated in Fig. 11-1 for studying diffusion rates of H_2 and N_2. The effective diffusivity is defined in terms of such rates (per unit of total cross-sectional area) by the equation

$$(N_A)_e = -D_e \frac{dC_A}{dr} = -\frac{p}{R_g T} D_e \frac{dy_A}{dr} \tag{11-19}$$

where the subscript e on N_A emphasizes that this is a diffusion flux in a porous catalyst rather than for a single pore, as given by Eq. (11-1). If we use the concentration-independent diffusivity D given by Eq. (11-4), D_e for a porous pellet will also be constant. Then Eq. (11-19) can be integrated to give

$$(N_A)_e = -\frac{p}{R_g T} D_e \frac{(y_A)_2 - (y_A)_1}{\Delta r} \tag{11-20}$$

where Δr is the length of the pellet. If the flow rates and concentrations are measured for the experiment pictured in Fig. 11-1, $(N_A)_e$ can be calculated. Then this flux and the measured concentrations and pellet length are substituted in Eq. (11-20) to obtain an experimental effective diffusivitv.

Dynamic methods have also been used to measure D_e. For example,†† a pulse input of diffusing component A can be inserted into a stream of helium flowing

† See R. C. Reid, J. M. Prausnitz, and T. K. Sherwood, "The Properties of Gases and Liquids," 3d ed., chap. 11, McGraw-Hill Book Company, New York, 1977.

‡ Takehiko Furusawa and J. M. Smith, *Ind. Eng. Chem. Fundam.*, 12, 197 (1979).

§ A summary up to 1969 is available in C. N. Satterfield, "Mass Transfer in Heterogeneous Catalysis," pp. 56–77, Massachusetts Institute of Technology Press, Cambridge, Mass., 1970. See also C. N. Satterfield and P. J. Cadle, *Ind. Eng. Chem., Fund. Quart.*, 7, 202 (1968); *Process Design Develop.*, 7, 256 (1968); L. F. Brown, H. W. Haynes, and W. H. Manogue, *J. Catalysis*, 14, 220 (1969).

¶ Originally proposed by E. Wicke and R. Kallenbach [*Kolloid-Z.*, 17, 135 (1941)].

†† Gulsen Dogu and J. M. Smith, *AIChE J.*, 21, 58 (1975).

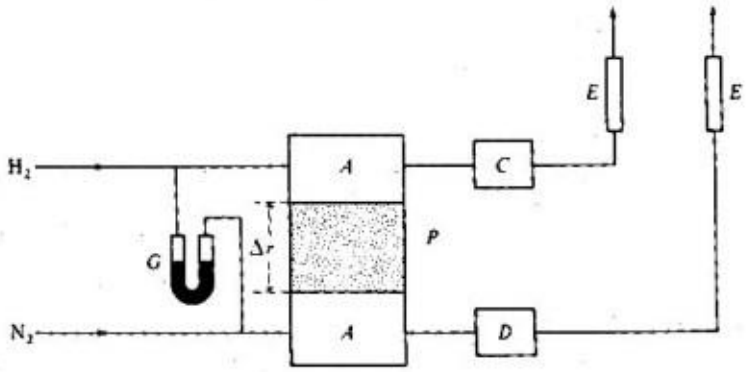

A – Mixing chambers
C – Detector for determining composition of N_2 in H_2 stream
D – Detector for determining composition of H_2 in N_2 stream
E – Flow meters
P – Catalyst pellet
G – Pressure equalization gauge

Figure 11-1 Constant-pressure apparatus for measuring diffusion rates in porous catalysts.

through the upper chamber, as indicated in Fig. 11-2. Pure helium also flows through the lower chamber. Some of the pulse of *A* diffuses through the pellet and is measured as a response pulse at the detector in the lower stream. For high flow rates of a nonadsorbing component, the effective diffusivity is given by

$$D_e = \frac{(\Delta r)^2 \varepsilon_p}{6\mu_1} \tag{11-21}$$

Here, μ_1 is the first moment (retention time) of the diffusing component in the pellet. It is obtained from the measured response pulse $C_A(t)$ by the equation

$$\mu_1 = \frac{\int_0^\infty C_A(t)t\,dt}{\int_0^\infty C_A(t)\,dt} \tag{11-22}$$

where $C_A(t)$ = concentration (function of time, t) in the response pulse
ε_p = porosity of pellet
Δr = length of pellet

Other equations have been developed,† both for adsorbing components and for lower flow rates across the pellet faces (see Prob. 11-5).

Comparison of diffusivities from steady-state and dynamic experiments can, in principle, provide information about pore structure. For example, dead-end pores should not affect diffusion at steady state, but would influence the results in dynamic experiments. Actually, uncertainties in accuracy of experimental results

† A. Burghardt and J. M. Smith, *Chem. Eng. Sci.*, **34**, 367 (1979) and Gulsen Dogu and J. M. Smith, *Chem. Eng. Sci.*, **23**, 123 (1976).

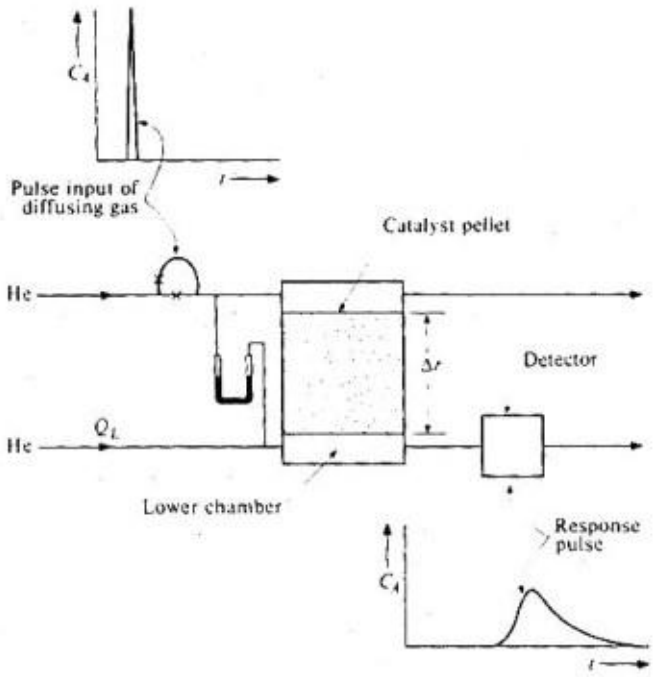

Figure 11-2 Dynamic method for measuring diffusivities in porous catalysts.

has prevented, as yet, meaningful comparisons. Another method of evaluating effective diffusivities, provided the rate equation for the chemical step is known, is comparison of the observed and predicted global rates by combining the equation for the chemical step with the intraparticle mass-transport resistance (see Example 11-9 for a variation of this method).

In the absence of experimental data it is necessary to estimate D_e from the physical properties of the catalyst. In this case the first step is to evaluate the diffusivity for a single cylindrical pore, that is, to evaluate D from Eq. (11-4). Then a geometric *model* of the pore system is used to convert D to D_e for the porous pellet. A model is necessary because of the complexity of the geometry of the void spaces. The optimum model is a realistic representation of the geometry of the voids (with tractable mathematics) that can be described in terms of easily measurable physical properties of the catalyst pellet. As noted in Chap. 8, these properties are the surface area and pore volume per gram, the density of the solid phase, and the distribution of void volume according to pore size.

The Parallel-pore Model Wheeler† proposed a model, based on the first three of these properties, to represent the monodisperse pore-size distribution in a catalyst

† A. Wheeler, in P. H. Emmett (ed.), "Catalysis," vol. II, chap. 2, Reinhold Publishing Corporation, New York, 1955; A. Wheeler, "Advances in Catalysis," vol. III, p. 250, Academic Press, Inc., New York, 1951.

pellet. From ρ_s and V_g the porosity ε_p is obtained from Eq. (8-9). Then a mean pore radius $\bar{a}$ is evaluated† by writing equations for the total pore volume and total pore surface in a pellet. The result, developed as Eq. (8-18), is

$$\bar{a} = \frac{2V_g}{S_g} \tag{11-23}$$

By using V_g, S_g, and ρ_s, Wheeler replaced the complex porous pellet with an assembly (having a porosity ε_p) of cylindrical pores of radius $\bar{a}$. To predict D_e from the model the only other property necessary is the length x_L of the diffusion path. If we assume that, on the average, the pore makes an angle of 45° with the coordinate r in the resultant direction of diffusion (for example, the radial direction in a spherical pellet), $x_L = \sqrt{2}\,r$. Owing to pore interconnections and noncylindrical shape, this value of x_L is not very satisfactory. Hence, it is customary to define x_L in terms of an adjustable parameter, the *tortuosity factor* δ, as follows:

$$x_L = \delta r \tag{11-24}$$

An effective diffusivity can now be predicted by combining Eq. (11-1) for a single pore with this parallel-pore mode. To convert D, which is based on the cross-sectional area of the pore, to a diffusivity based upon the total area perpendicular to the direction of diffusion, D should be multiplied by the porosity. In Eq. (11-1), x is the length of a single, straight cylindrical pore. To convert this length to the diffusion path in a porous pellet, x_L from Eq. (11-24) should be substituted for x. With these modifications the diffusive flux in the porous pellet will be

$$(N_A)_e = -\frac{p}{R_g T}\frac{\varepsilon D}{\delta}\frac{dy_A}{dr} \tag{11-25}$$

Comparison with Eq. (11-19) shows that the effective diffusivity is

$$D_e = \frac{\varepsilon D}{\delta} \tag{11-26}$$

where D is given (in the absence of surface diffusion) by Eq. (11-4). The use of Eq. (11-26) to predict D_e is somewhat limited because of the uncertainty about δ. Comparison of D_e from Eq. (11-26) with values obtained from experimental data for various catalysts using Eq. (11-20) shows that δ varies from less than unity to more than 6.‡

The Random-pore Model This model was originally developed for pellets containing a bidisperse pore system, such as the alumina described in Chap. 8 (Fig. 8-8). It is supposed that the pellet consists of an assembly of small particles. When the

† Recall from Sec. 8-3 that regardless of the complexity of the void structure, it is assumed that the void spaces may be regarded as cylindrical pores.

‡ Tortuosity factors less than unity can occur when the surface diffusion is significant. This is because D_e is increased, while D as defined in Eq. (11-4) does not include this contribution. See Sec. 11-4 for a corrected D to include surface diffusion. C. N. Satterfield ("Mass Transfer in Heterogeneous Catalysis," Massachusetts Institute of Technology Press, Cambridge, Mass., 1970) has summarized data from the literature and recommended the use of $\delta = 4$ when surface diffusion is insignificant. See also P. Carman, *Trans. Inst. Chem. Engrs.*, **15**, 150 (1937).

particles themselves contain pores (micropores), there exists both a macro and a micro void-volume distribution. The voids are not imagined as capillaries, but more as an assembly of short void regions surrounding and between individual particles, as indicated in Fig. 11-3. The nature of the interconnection of macro and micro void regions is the essence of the model. Transport in the pellet is assumed to occur by a combination of diffusion through the macro regions (of void fraction ε_M), the micro regions (of void fraction ε_μ), and a series contribution involving both regions. It is supposed that both micro and macro regions can be represented as straight, short cylindrical pores of average radii $\bar{a}_M$ and $\bar{a}_\mu$. The magnitude of the individual contributions is dependent on their effective cross-sectional areas (perpendicular to the direction of diffusion). The details of the development are given elsewhere,† but in general these areas are evaluated from the probability of pore interconnections. The resultant expression for D_e may be written

$$D_e = \bar{D}_M \varepsilon_M^2 + \frac{\varepsilon_\mu^2(1 + 3\varepsilon_M)}{1 - \varepsilon_M} \bar{D}_\mu \tag{11-27}$$

Here $\bar{D}_M$ and $\bar{D}_\mu$ are obtained by applying Eq. (11-4) to macro and micro regions. Thus

$$\frac{1}{\bar{D}_M} = \frac{1}{\mathscr{D}_{AB}} + \frac{1}{(\bar{\mathscr{D}}_K)_M} \tag{11-28}$$

$$\frac{1}{\bar{D}_\mu} = \frac{1}{\mathscr{D}_{AB}} + \frac{1}{(\bar{\mathscr{D}}_K)_\mu} \tag{11-29}$$

No tortuosity factor is involved in this model.‡ The actual path length is equal to the distance coordinate in the direction of diffusion. To apply Eq. (11-27)

† N. Wakao and J. M. Smith, *Chem. Eng. Sci.*, **17**, 825 (1962); *Ind. Eng. Chem., Fund. Quart.*, **3**, 123 (1964).

‡ Thus the random-pore model does not involve an adjustable parameter.

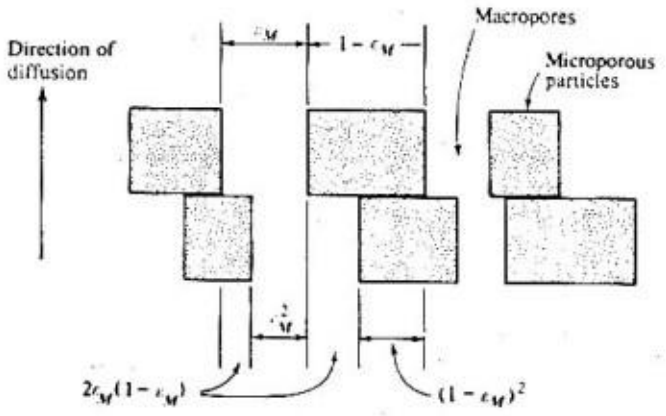

Figure 11-3 Random-pore model.

requires void fractions and mean pore radii for both macro and micro regions. The mean pore radii can be evaluated for the micro region by applying Eq. (11-23) to this region. However, $\bar{a}_M$ must be obtained from the pore-volume distribution, as described in Sec. 8-7. The mean pore radii are necessary in order to calculate $(\mathscr{D}_K)_M$ and $(\mathscr{D}_K)_\mu$ from Eqs. (11-28) and (11-29).

The random-pore model can also be applied to monodisperse systems. For a pellet containing only macropores, $\varepsilon_\mu = 0$ and Eq. (11-27) becomes

$$D_e = \bar{D}_M \varepsilon_M^2 \tag{11-30}$$

Similarly, for a material such as silica gel, where $\varepsilon_M = 0$, the effective diffusivity is

$$D_e = \bar{D}_\mu \varepsilon_\mu^2 \tag{11-31}$$

Comparison of these last two equations with Eq. (11-26) indicates that $\delta = 1/\varepsilon$. The significance of the random-pore model is that the effective diffusivity is proportional to the square of the porosity. This has also been proposed by Weisz and Schwartz.† Johnson and Stewart‡ have developed another method for predicting D_e that utilizes the pore-volume distribution. Evaluation of their model and the random-pore model with extensive experimental data has been carried out by Satterfield and Cadle§ and Brown et al.¶

The examples that follow illustrate the methods that have been outlined for evaluating D_e from experimental data and predicting it from a pore model.

Example 11-4 Rothfeld †† has measured diffusion rates for isobutane, in the isobutane-helium system, through a $\frac{1}{8}$-in.-long pelleted cylinder of alumina (diameter $\frac{1}{8}$ in.). The measurements were at 750 mmHg total pressure and 25°C, and the diffusion direction was through the pellet parallel to the central axis. The following data are available:

$$S_g = 76 \text{ m}^2/\text{g}$$

$$\varepsilon_M = 0.18 \qquad \varepsilon_\mu = 0.34$$

$$\bar{a}_M = 4800 \text{ Å} \qquad \bar{a}_\mu = 84 \text{ Å}$$

The mole fraction of isobutane is 1.0 on one face of the pellet and zero on the other face. The experimental results gave

$$\frac{(N_A)_e R_g T \Delta r}{\mathscr{D}_{AB} P_t (y_2 - y_1)} = -0.023$$

where N_A is the diffusion flux of isobutane and $\mathscr{D}_{AB}$ is the bulk diffusivity in the isobutane-helium system.

† P. B. Weisz and A. B. Schwartz, *J. Catalysis*, **1**, 399 (1962).

‡ M. F. L. Johnson and W. E. Stewart, *J. Catalysis*, **4**, 248 (1965).

§ C. N. Satterfield and P. J. Cadle, *Ind. Eng. Chem., Fund. Quart.*, **7**, 202 (1968); *Process Design Develop.*, **7**, 256 (1968).

¶ L. F. Brown, H. W. Haynes, and W. H. Manogue, *J. Catalysis*, **14**, 220 (1969).

†† L. B. Rothfeld, *AIChE J.*, **9**, 19 (1963).

(*a*) Calculate the experimental value of D_e. (*b*) What macropore tortuosity factor is indicated by the data? What is δ_M predicted by the random pore model?

SOLUTION (*a*) According to the procedure of Example 11-1 (the Chapman-Enskog equation), the bulk diffusivity in the isobutane-helium system at 750 mmHg pressure and 25°C is

$$\mathscr{D}_{AB} = 0.313 \text{ cm}^2/\text{s}$$

Thus the measured diffusion flux of isobutane is

$$(N_A)_e = \frac{-0.023(0.313)(\frac{750}{760})(0 - 1.0)}{82(25 + 273)\frac{1}{8}(2.54)} = 9.1 \times 10^{-7} \text{ g mol/(s)(cm}^2\text{)}$$

This value of $(N_A)_e$ can be used in Eq. (11-20) to calculate the experimental D_e,

$$D_e = -\frac{(N_A)_e R_g T \Delta r}{p(y_2 - y_1)} = \frac{-9.1 \times 10^{-7}(82)(298)(\frac{1}{8})(2.54)}{\frac{750}{760}(0 - 1.0)} = 0.0072 \text{ cm}^2/\text{s}$$

(*b*) The *parallel-pore* model is designed for a *monodisperse* pore system and hence is not directly applicable to this catalyst. Since the macropores are much larger than the micropores, an approximate approach is to neglect the contribution of the micropores to the mass transport. Using the macro properties in Eq. (11-26) and the experimental D_e, we have

$$D_e = 0.0072 = \frac{\varepsilon_M \bar{D}_M}{\delta_M} = \frac{0.18\bar{D}_M}{\delta_M}$$

or

$$\delta_M = \frac{0.18\ \bar{D}_M}{0.0072}$$

The combined diffusivity in the macropores is given by Eq. (11-28)

$$\frac{1}{\bar{D}_M} = \frac{1}{\mathscr{D}_{AB}} + \frac{1}{(\bar{D}_K)_M}$$

From Eq. (11-17),

$$(\mathscr{D}_K)_M = 9.70 \times 10^3(4{,}800 \times 10^{-8})\left(\frac{298}{58.1}\right)^{1/2} = 1.10 \text{ cm}^2/\text{s}$$

$$\frac{1}{\bar{D}_M} = \frac{1}{0.313} - \frac{1}{1.10}$$

$$\bar{D}_M = 0.243 \text{ cm}^2/\text{s}$$

Then the tortuosity factor suggested by the data is

$$\delta_M = \frac{0.18(0.243)}{0.0072} = 6.1$$

If we assume that all the diffusion is in the macropores, Eq. (11-30) gives D_e for the *random-pore model*. Combining Eq. (11-30) with Eq. (11-26) yields

$$\frac{\varepsilon_M \bar{D}_M}{\delta_M} = D_e = \bar{D}_M \varepsilon_M^2$$

or

$$\delta_M = \frac{1}{\varepsilon_M} = \frac{1}{0.18} = 5.5$$

in reasonable agreement with the experimental result. Actually, this pellet is relatively dense (low ε_M) and probably was prepared with a high pelleting pressure. Hence the diffusion likely is affected by the micropores.†

Example 11-5 Vycor (porous silica) appears to have a pore system with fewer interconnections than alumina. The pore system is monodisperse, with the somewhat unusual combination of a small mean pore radius (45 Å) and a low porosity 0.31. Vycor may be much closer to an assembly of individual voids than to an assembly of particles surrounded by void spaces. Since the random-pore model is based on the assembly-of-particles concept, it is instructive to see how it applies to Vycor. Rao and Smith‡ measured an effective diffusivity for hydrogen of 0.0029 cm^2/s in Vycor. The apparatus was similar to that shown in Fig. 11-1, and data were obtained using an H_2—N_2 system at 25°C and 1 atm. Predict the effective diffusivity by the random-pore model.

SOLUTION Only micropores are present, and so D_e should be predicted by means of Eq. (11-31). Furthermore, mass transport in the small pores will be predominately by Knudsen diffusion. Hence $\bar{D}_\mu = (\bar{\mathscr{D}}_K)_\mu$, from Eq. (11-29). and

$$D_e = (\bar{\mathscr{D}}_K)_\mu \varepsilon_\mu^2$$

$$(\bar{\mathscr{D}}_K)_\mu = 9.7 \times 10^3 (45 \times 10^{-8}) \left(\frac{298}{2.02}\right)^{1/2} = 0.053 \text{ cm}^2/\text{s}$$

Then the predicted D_e is

$$D_e = 0.053(0.31)^2 = 0.0050 \text{ cm}^2/\text{s}$$

This value is 70% greater than the experimental result—evidence that the random-pore model is not very suitable for Vycor.

† W. Wakao and J. M. Smith [*Chem. Eng. Sci.*, **17**, 825 (1962)] analyzed the diffusion data of Rothfeld. These data were obtained in an apparatus of the type shown in Fig. 11-1. For the butane-helium system this means that N_{He}/N_{C_4} is 3.80. Diffusion is far from equimolal, suggesting that Eqs. (11-28) and (11-29) for D values are not exact. For this particular case Eq. (11-2) should be used. In most reaction systems the counterdiffusion of reactants and products is much closer to equimolal, so that Eqs. (11-28) and (11-29) are better approximations.

‡ M. J. Rao and J. M. Smith, *AIChE J.*, **10**, 243 (1964).

The experimental tortuosity, from Eq. (11-26), is

$$\delta = \frac{0.31\bar{D}_u}{D_e} = \frac{0.31(\mathscr{D}_K)_u}{D_e} = \frac{0.31(0.053)}{0.0029} = 5.6$$

In contrast, the tortuosity predicted by the random-pore model would be $1/\varepsilon = 3.2$.

Silica gel of large surface area has even smaller pores than Vycor, but a larger void fraction; for example, for one grade of silica gel $\varepsilon = 0.486$ and $\bar{a} = 11$ Å. Schneider† studied the diffusion of ethane in this material at 200°C (at this temperature surface diffusion was negligible) and found an effective diffusivity such that δ from Eq. (11-26) was 3.34. The value predicted from the random-pore model is $1/\varepsilon = 2.1$. Note that the Wheeler model would predict $\delta = \sqrt{2}$ for Vycor, silica gel, or other porous material.

A final word should be said about the variety of porous materials. Porous catalysts cover a rather narrow range of possibilities. Perhaps the largest variation is between monodisperse and bidisperse pellets, but even these differences are small in comparison with materials such as freeze-dried beef, which is like an assembly of solid fibers, and freeze-dried fruit, which appears to have a structure like an assembly of ping-pong balls with holes in the surface to permit a continuous void phase.‡ Also for sintered pellets, where pore interconnections have been greatly reduced by heating, tortuosity factors as high as 100 have been measured.§

11-4 Surface Diffusion

Surface migration is pertinent to a study of intrapellet mass transfer if its contribution is significant with respect to diffusion in the pore space at reaction temperature. When multimolecular-layer adsorption occurs, surface diffusion has been explained as a flow of the outer layers as a condensed phase.¶ However, surface transport of interest in relation to catalytic reaction occurs in the monomolecular layer. It is more appropriate to consider, as proposed by deBoer,†† that such transport is an activated process, dependent on surface characteristics as well as those of the adsorbed molecules. Imagine that a molecule in the gas phase strikes the pore wall and is adsorbed. Then two alternatives are possible: desorption into the gas or movement to an adjacent active site on the pore wall (surface diffusion). If desorption occurs, the molecule can continue its journey in the void space of the pore or be readsorbed by again striking the wall. In moving along the wall, the same molecule would be transported sometimes on the surface and sometimes in the gas phase. If this view is correct, the relative contribution of surface migration

† Petr Schneider and J. M. Smith, *AIChE J.*, 14, 886 (1968).

‡ J. C. Harper, *AIChE J.*, 8, 298 (1962).

§ J. H. Krasuk and J. M. Smith, *AIChE J.*, 18, 506 (1972).

¶ D. H. Everett in F. S. Stone (ed.), Structure and Properties of Porous Materials, *Proc. Tenth Symp. Colston Res. Soc.*, Butterworth, London, p. 178, 1958.

†† J. H. deBoer, in "Advances in Catalysis," vol. VIII, p. 18, Academic Press, Inc., New York, 1959.

would increase as the surface area increases (or the pore size decreases). There is evidence to indicate that such is the case.†

Experimental verification of surface diffusion is usually indirect, since concentrations of adsorbed molecules on a surface are difficult to measure. When gas concentrations are obtained, the problem arises of separating the surface and pore-volume transport rates. One solution is to measure both N_A and N_B in the apparatus shown in Fig. 11-1, using a nonadsorbable gas for A. If the diffusion rate of B is greater than that calculated from N_A by Eq. (11-8), the excess is attributable to surface migration. Barrer and Barrie‡ used this procedure with Vycor at room temperature and found surface migration significant for such gases as CO_2, CH_4, and C_2H_4 and negligible for helium and hydrogen. Rivarola§ found that for CO_2 the surface contribution on an alumina pellet increased from 3.5 to 54% of the total mass-transfer rate as the macropore properties changed from $\bar{a}_M = 1{,}710$ Å and $\varepsilon_M = 0.33$ to $\bar{a}_M = 348$ Å and $\varepsilon_M = 0.12$.

By analogy to Fick's law, a surface diffusivity $\mathscr{D}_s$ may be defined in terms of a surface concentration C_s in moles of adsorbate per square centimeter of surface:

$$N_s = -\mathscr{D}_s \frac{dC_s}{dx} \tag{11-32}$$

where N_s is the molal rate per unit perimeter of pore surface. In order to combine surface and pore-volume contributions in a *catalyst pellet*, the surface flux should be based on the total area of the catalyst perpendicular to diffusion and on the coordinate r. If this flux is $(N_s)_c$, then

$$(N_s)_c = -D_s \rho_p \frac{d\bar{C}}{dr} \tag{11-33}$$

where ρ_p is the density of the catalyst and $\bar{C}$ now represents the moles adsorbed per gram of catalyst.§ To be useful, Eq. (11-33) must be expressed in terms of the concentration in the gas phase. If the adsorption step is fast with respect to surface transfer from site to site on the catalyst, we may safely assume equilibrium between gas and surface concentration. Otherwise the relation between the two concentrations depends on the intrinsic rates of the two processes.¶ If equilibrium is assumed, and if the isotherm is linear, then

$$\bar{C}_A = (K_A \bar{C}_m) C_g = K'_A \frac{p y_A}{R_g T} \tag{11-34}$$

where the subscript A refers to the adsorbate and K' is the linear form of the equilibrium constant, in cubic centimeters per gram. The latter is obtained from

† J. B. Rivarola and J. M. Smith, *Ind. Eng. Chem., Fund. Quart.*, 3, 308 (1964).

‡ R. M. Barrer and J. M. Barrie, *Proc. Roy. Soc. (London)*, A213, 250 (1952).

§ To relate $\mathscr{D}_s$ and D_s requires a model for the porous structure. The parallel-pore and random-pore models have been applied to surface diffusion by J. H. Krasuk and J. M. Smith [*Ind. Eng. Chem., Fund. Quart.*, 4, 102 (1965)] and J. B. Rivarola and J. M. Smith [*Ind. Eng. Chem., Fund. Quart.*, 3, 368 (1964)].

¶ J. A. Moulijn, et al. [*Ind. Eng. Chem. Fundam.* 16, 301 (1077)] have extended the theory of intraparticle diffusion to allow for finite rates of surface diffusion.

the Langmuir isotherm, Eq. (7-15), when adsorption is small enough that the linear form is valid. Now, applying Eq. (11-33) to component A,

$$(N_s)_r = -\frac{p}{R_g T}\rho_p K'_A D_s \frac{dy_A}{dr} \tag{11-35}$$

Equation (11-35) gives the surface diffusion of A in the same form as Eq. (11-19) applied earlier to transport in the gas phase of the pores. From these equations the total flux and total effective diffusivity are given by

$$(N_A)_t = -\frac{p}{R_g T}(D_e + \rho_p K'_A D_s)\frac{dy_A}{dr} \tag{11-36}$$

$$(D_e)_t = D_e + \rho_p K'_A D_s \tag{11-37}$$

If the density of the catalyst and the adsorption equilibrium constant are known, Eq. (11-37) permits the evaluation of a total effective diffusivity from D_s. Data for D_s have been reported in the literature in a variety of ways, depending on the definitions of adsorbed concentrations and equilibrium constants. Schneider† has summarized much of the information for light hydrocarbons on various catalysts in the form defined by Eq. (11-35). Such D_s values ranged from 10^{-3} to 10^{-6}, depending on the nature of the adsorbent and the amount adsorbed. Most values were in the interval 10^{-4} to 10^{-5} cm^2 s. Data for other adsorbates‡ have similar magnitudes and show that the variation with adsorbed concentration can be large.

The effect of temperature on D_s, given an activated process, is described by an Arrhenius-type expression,

$$D_s = \mathrm{A}e^{-E_s/R_g T}$$

where E_s is the activation energy for surface diffusion. The variation of K'_A with temperature is given by van't Hoff equation

$$\frac{d \ln K'_A}{dT} = \frac{\Delta H}{R_g T^2}$$

or

$$K'_A = \mathrm{A}'e^{-\Delta H/R_g T}$$

The observed rate of surface diffusion, according to Eq. (11-35), will be proportional to the product $K'_A D_s$. Substituting the above expressions for K'_A and D_s in Eq. (11-35),

$$(N_s)_r = -\frac{p}{R_g T}\rho_p(\mathrm{AA}')e^{-(1/R_g T)(\Delta H - E_s)}\frac{dy_A}{dr}$$

† Petr Schneider and J. M. Smith, *AIChE J.*, **14**, 886 (1968).

‡ R. A. W. Haul, *Angew. Chem.*, **62**, 10 (1950); P. S. Carman and F. A. Raal, *Proc. Roy. Soc. (London)*, **209A**, 38 (1951); *Trans. Faraday Soc.*, **50**, 842 (1954); D. H. Everett in F. S. Stone (ed.), Structure and Properties of Porous Materials, *Proc. Tenth Symp. Colston Res. Soc.*, Butterworth, London, p. 178, 1958.

The exponential term expresses a much stronger temperature dependency than the coefficient $1/T$. If we neglect the latter, we may express the *temperature* effect on the rate as

$$(N_s)_e = -\mathrm{A}'' e^{-(1/R_g T)(\Delta H + E_s)}$$

where

$$\mathrm{A}'' = \mathrm{A}\mathrm{A}' \frac{dy_A}{dr} \frac{p}{R_g T} \rho_p$$

This equation shows that the observed or apparent activation energy for surface diffusion is related to E_s by

$$E' = \Delta H + E_s \tag{11-38}$$

From available data† it appears that E_s is only a few kilocalories per mole. The heat of adsorption ΔH is generally greater than this, particularly for chemisorption, and is always negative. Therefore the observed effect is a decrease in rate of surface diffusion with increase in temperature. Note that ΔH is negative.

From the assumptions and approximations presented, it is clear that surface diffusion is not well understood. It is hoped that improved interpretations of surface migration will permit a more accurate assessment of its effect on global rates of reaction. When we consider the effect of intraparticle resistances in Secs. 11-7 to 11-12 we shall suppose that the D_e used is the most appropriate value and includes, if necessary, a surface contribution.

INTRAPELLET HEAT TRANSFER

11-5 Concept of Effective Thermal Conductivity

The effective thermal conductivities of catalyst pellets are surprisingly low. Therefore significant intrapellet temperature gradients can exist, and the global rate may be influenced by thermal effects. The effective conductivity is the energy transferred per unit of *total* area of pellet (perpendicular to the direction of heat transfer). The defining equation, analogous to Eq. (11-19) for mass transfer, may be written

$$Q_e = -k_e \frac{dT}{dr} \tag{11-39}$$

where Q_e is the rate of energy transfer per unit of total area.

A major factor contributing to small values of k_e is the numerous void spaces that hinder the transport of energy. In addition, the path through the solid phase offers considerable thermal resistance for many porous materials, particularly pellets made by compressing microporous particles. Such behavior is readily understood if these materials are viewed as an assembly of particles which contact each other only through adjacent points. There is strong experimental evidence that such point contacts are regions of high thermal resistance. For example, the

† Petr Schneider and J. M. Smith, *AIChE J.*, 14, 886 (1968).

thermal conductivity of the bulk solid (zero porosity) from which the particles are prepared does not have a large effect on k_e. Masamune† found that the effective thermal conductivity of pellets of microporous particles of silver was only two to four times that of alumina pellets, at the same macropore void fraction, pressure, and temperature. In contrast, the thermal conductivity of solid silver is about 200 times as large as that of solid alumina. Furthermore, k_e is a strong function of the void fraction, increasing as ε_p decreases. Materials such as alumina pellets may be regarded as a porous assembly within a second porous system. Each particle from which the pellet is made contains a microporous region. These particles are in point contact with like particles and are surrounded by macroporous regions. When viewed in this way, the thermal conductivity of the bulk solid should have little influence on k_e.

The pressure and nature of the fluid in the pores has an effect on the effective thermal conductivity. With liquids the effect of pressure is negligible and k_e is of the same magnitude as the true conductivity of the liquid. For gases at low pressures, where the mean free path is the same or larger than the pore size, free-molecule conduction controls the energy transfer. In this region k_e increases with pressure. At higher pressures k_e is about independent of pressure. The transition pressure depends on the gas as well as on the pore size. For air the transition pressure is about 470 mm in a silver pellet with mean pore diameter of 1500 Å. For helium the value would be above 760 mm.† For alumina pellets, at 120°F and a macropore void fraction of $\varepsilon_M = 0.40$, k_e was 0.050 in vacuum, 0.082 with pores filled with air, and 0.104 Btu/(h)(ft)(°F) with helium, at atmospheric pressure.‡ Temperature does not have a strong influence. The effect is about what would be expected for the combination of variations of thermal conductivity with temperature for the solid and fluid phases.

11-6 Effective Thermal-Conductivity Data

Most of the experimental information on k_e for catalyst pellets is described by Masamune and Smith.† Mischke and Smith‡ and Sehr.§ Sehr gives single values for commonly used catalysts. The other two works present k_e as a function of pressure, temperature, and void fraction for silver and alumina pellets. Both transient and steady-state methods have been employed. Figure 11-4 shows the variation of k_e with pellet density and temperature for alumina (boehmite, $Al_2O_3 \cdot H_2O$) pellets. Different densities were obtained by increasing the pressure used to pellet the microporous particles. The data are at vacuum conditions and therefore represent the conduction of the solid matrix of the pellet. Note how low k_e is in comparison with the thermal conductivity of solid alumina [about 1.0 Btu/(h)(ft)(°F)]. The low value is due to the small heat-transfer areas at the point-to-point contacts between particles. As the pelleting pressure increases (lower macropore void fraction), these contact areas increase, and so does k_e. Figure 11-5 shows the effect of macropore void fraction on k_e for pellets of microporous silver

† S. Masamune and J. M. Smith, *J. Chem. Eng. Data*, 8, 54 (1963).
‡ R. A. Mischke and J. M. Smith, *Ind. Eng. Chem., Fund. Quart.*, 1, 288 (1962).
§ R. A. Sehr, *Chem. Eng. Sci.*, 2, 145 (1958).

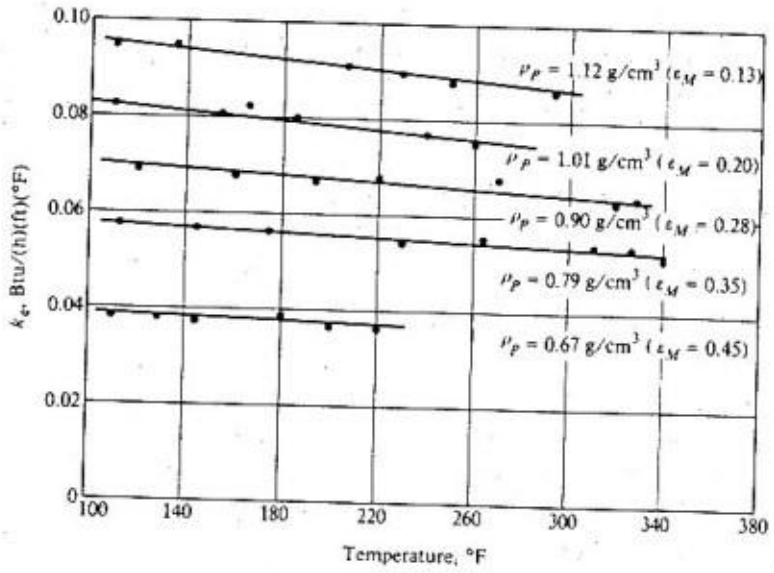

Figure 11-4 Effective thermal conductivity of alumina (boehmite) catalyst pellets at 10 to 25 microns Hg pressure.

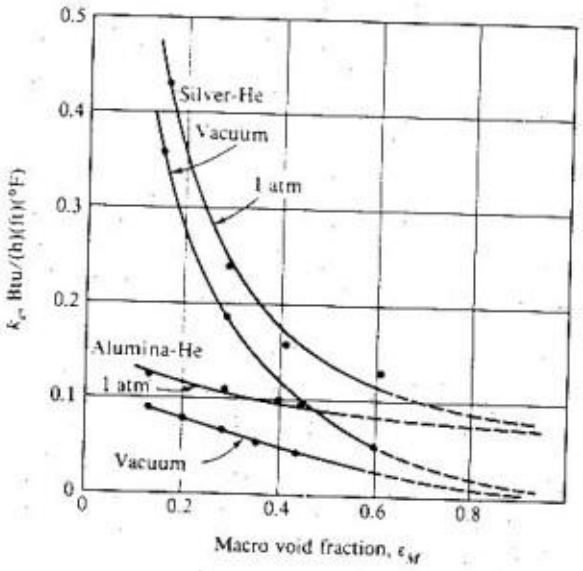

Figure 11-5 Effect of macropore void fraction on k_e at 34°C.

and microporous alumina (boehmite) particles. Data are given for two conditions: vacuum and pores filled with helium at 1 atm, both at 34°C. Since helium has a high conductivity, the two curves would encompass the values expected for any reaction mixture. As 1 atm is at or beyond the transition pressure, increasing the pressure would have little effect (until the thermodynamic critical point is approached). Similarly, silver and boehmite represent close to the extremes of conductivity for the solids that might be expected in porous catalysts. Figure 11-6 is a similar plot of data for three cases: vacuum, air-filled pores at 1 atm pressure, and helium-filled pores at 1 atm pressure. These results are for boehmite pellets.†

The theory of heat transfer in porous materials has not been developed to the level of that for mass transfer. The contribution of the solid phase makes the problem more complex. It is not yet possible to predict k_e accurately from the properties of the fluid and solid phases. Butt‡ has applied and extended the random-pore model to develop a valuable method of predicting the effects of void fraction, pressure, and temperature on k_e. A different and more approximate approach§ proposes that the effective thermal conductivity is a function only of

† R. A. Mischke and J. M. Smith, *Ind. Eng. Chem., Fund. Quart.*, 1, 288 (1962).
‡ J. B. Butt, *AIChE J.*, 11, 106 (1965).
§ W. Woodside and J. H. Messmer, *J. Appl. Phys.*, **32**, 1688 (1961).

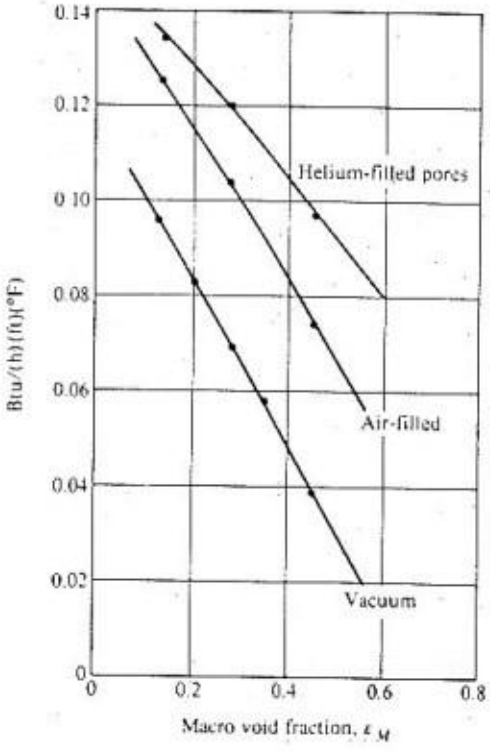

Figure 11-6 Effective thermal conductivity of alumina (boehmite) pellets vs. void fraction at 120°F.

the volume fraction of the void phase and the thermal conductivities of the bulk-fluid and solid phases, k_f and K_s. The relationship is

$$k_e = k_s\left(\frac{k_f}{k_s}\right)^{1-\epsilon} \tag{11-40}$$

In spite of the difficulties in predicting k_e, it is still possible to choose a value which will be reasonably correct, because the possible range of values (excluding vacuum conditions) is only from about 0.1 to 0.4 Btu/(h)(ft)(°F). Furthermore, the nature of the variations within this range that are due to void fraction, temperature, and pressure are known approximately from Figs. 11-4 to 11-6.

MASS TRANSFER WITH REACTION

After discussing the effective transport coefficients D_e and k_e, we now turn to the main objective of the chapter: an expression of the rate of reaction for the whole catalyst pellet,† $\mathbf{r}_P$, in terms of the temperature and concentrations existing at the *outer* surface. We start in a formal way by defining an effectiveness factor η as follows:

$$\eta = \frac{\text{actual rate for the whole pellet}}{\text{rate evaluated at outer surface conditions}} = \frac{\mathbf{r}_P}{\mathbf{r}_s} \tag{11-41}$$

The equation for the local rate (per unit mass of catalyst) as developed in Chap. 9 may be expressed functionally as $\mathbf{r} = f(C, T)$, where C represents, symbolically, the concentrations of all the involved components.‡ Then Eq. (11-41) gives for $\mathbf{r}_P$

$$\mathbf{r}_P = \eta \mathbf{r}_s = \eta f(C_s, T_s) \tag{11-42}$$

With the formulation of Eq. (11-42) the objective becomes the evaluation of η rather than $\mathbf{r}_P$. Once η is known, Eq. (11-42) gives the rate for the whole pellet in terms of the temperature and concentration at the outer surface. Then the rate can be expressed in terms of the temperature and concentration of the bulk fluid by accounting for external resistances (Chap. 10). The effectiveness factor is a function of k_e, D_e, and the rate constants associated with the chemical step at the site, i.e., the constants in the rate equations developed in Chap. 9. In the remainder of this chapter we shall develop the relationship between η and these rate parameters. In Secs. 11-7 to 11-10 isothermal conditions are assumed. With this restraint k_e is not involved, and Eq. (11-42) becomes

$$\mathbf{r}_P = \eta f(C_s) \tag{11-43}$$

The nonisothermal problem is considered in Secs. 11-11 and 11-12.

† $\mathbf{r}_P$ is the rate for the whole pellet, but based on a unit mass of catalyst. The description "whole pellet" is used to denote that intrapellet effects are accounted for in $\mathbf{r}_P$. If the rate measured for one or more pellets is r and the mass of the pellets is m, then $\mathbf{r}_P = r\,m$.

‡ For example, for the reaction $A + B \rightleftarrows C$, Eq. (9-21) indicates that $f(C, T)$ would be

$$f(C, T) = k_s C_{\infty} K_A K_B \frac{C_A C_B - (1/K)(C_C)}{(1 + K_A C_A + K_B C_B + K_C C_C)^2}$$

where k and all the K values are functions of temperature.

11-7 Effectiveness Factors

Suppose that an irreversible reaction $A \rightarrow B$ is first order, so that for isothermal conditions $\mathbf{r} = f(C_A) = k_1 C_A$. Then Eq. (11-43) becomes

$$r_p = \eta k_1 (C_A)_s \tag{11-44}$$

We want to evaluate η in terms of D_e and k_1. The first step is to determine the concentration profile of A in the pellet. This is shown schematically in Fig. 11-7 for a spherical pellet (also shown is the external profile from C_b to C_s). The differential equation expressing C_A vs. r is obtained† by writing a mass balance over the spherical-shell volume of thickness Δr (Fig. 11-7). According to Eq. (3-1) at steady state the rate of diffusion into the element‡ less the rate of diffusion out will equal the rate of disappearance of reactant within the element. This rate will be $\rho_p k_1 C_A$ per unit volume, where ρ_p is the density of the pellet. Hence the balance may be written, omitting subscript A on C,

$$\left(-4\pi r^2 D_e \frac{dC}{dr}\right)_r - \left(-4\pi r^2 D_e \frac{dC}{dr}\right)_{r+\Delta r} = 4\pi r^2 \, \Delta r \rho_p k_1 C \tag{11-45}$$

† This development was first presented by A. Wheeler in W. G. Frankenburg, V. I. Komarewsky, and E. K. Rideal (eds.), "Advances in Catalysis," vol. III, p. 297, Academic Press, Inc., New York, 1951; see also P. H. Emmett (ed.), "Catalysis," vol. II, p. 133, Reinhold Publishing Corporation, New York, 1955.

‡ The diffusive flux into the element is given by Eq. (11-19). Note that for $A \rightarrow B$ there is equimolal counterdiffusion of A and B ($\alpha = 0$). The rate of diffusion is the product of the flux and the area, $4\pi r^2$.

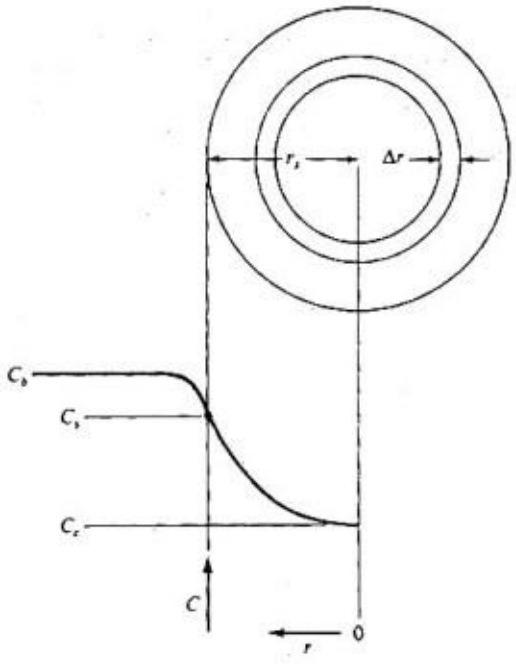

Figure 11-7 Reactant (A) concentration vs. position for first-order reaction on a spherical catalyst pellet.

If we take the limit as $\Delta r \to 0$ and assume that the effective diffusivity is independent of the concentration of reactant (see Sec. 11-2), this difference equation becomes

$$\frac{d^2C}{dr^2} + \frac{2}{r}\frac{dC}{dr} - \frac{k_1\rho_P}{D_e}C = 0 \tag{11-46}$$

At the center of the pellet symmetry requires

$$\frac{dC}{dr} = 0 \qquad \text{at } r = 0 \tag{11-47}$$

and at the outer surface

$$C = C_s \qquad \text{at } r = r_s \tag{11-48}$$

Linear differential equation (11-46) with boundary conditions (11-47) and (11-48) may be solved by conventional methods to yield

$$\frac{C}{C_s} = \frac{r_s}{r}\frac{\sinh\,(3\Phi_s r/r_s)}{\sinh\,3\Phi_s} \tag{11-49}$$

where Φ_s is a dimensionless group (a Thiele-type modulus for a *spherical* pellet) defined by

$$\Phi_s = \frac{r_s}{3}\sqrt{\frac{k_1\rho_P}{D_e}} \tag{11-50}$$

The second step is to use the concentration profile given by Eq. (11-49) to evaluate the rate of reaction $\mathbf{r}_P$ for the whole pellet. We have two choices for doing this: calculating the diffusion rate of reactant *into* the pellet at r_s, or integrating the local rate over the whole pellet. Choosing the first approach,

$$\mathbf{r}_P = \frac{1}{m_P}4\pi r_s^2 D_e\left(\frac{dC}{dr}\right)_{r=r_s} = \frac{3}{r_s\rho_P}D_e\left(\frac{dC}{dr}\right)_{r=r_s}$$

where the mass of the pellet is $m_P = \frac{4}{3}\pi r_s^3\rho_P$. Then, from Eq. (11-44),

$$\eta = \frac{3D_e}{r_s\rho_P k_1 C_s}\left(\frac{dC}{dr}\right)_{r=r_s} \tag{11-51}$$

Differentiating Eq. (11-49), evaluating the derivative at $r = r_s$, and substituting this into Eq. (11-51) gives

$$\eta = \frac{1}{\Phi_s}\left(\frac{1}{\tanh\,3\Phi_s} - \frac{1}{3\Phi_s}\right) \tag{11-52}$$

If this equation for the effectiveness factor is used in Eq. (11-44), the desired rate for the whole pellet in terms of the *concentration at the outer surface* is

$$\mathbf{r}_P = \frac{1}{\Phi}\left(\frac{1}{\tanh\,3\Phi_s} - \frac{1}{3\Phi_s}\right)k_1 C_s \tag{11-53}$$

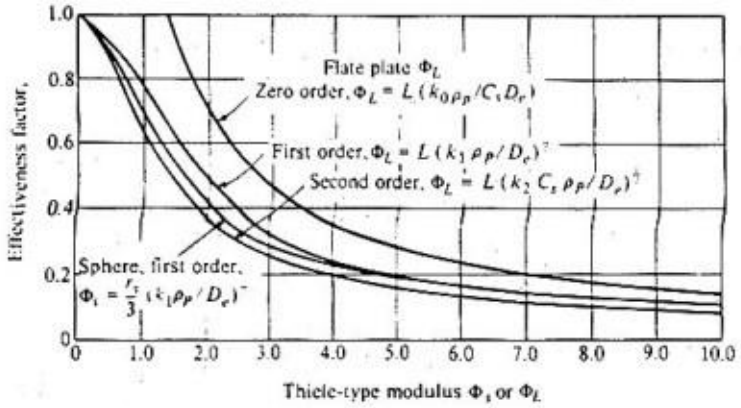

Figure 11-8 Effectiveness factor for various pellet shapes and kinetic equations.

Both D_e and k_1 are necessary to use Eq. (11-53). The relative importance of diffusion and chemical-reaction processes is evident from Eq. (11-52), which is represented by the second-lowest curve in Fig. 11-8. This curve shows that for small values of Φ_s, $\eta \to 1$. Then intraparticle mass transport has no effect on the rate per pellet; the chemical step controls the rate. From Eq. (11-50), small values of Φ_s are obtained when the pellets are small, the diffusivity is large, or the reaction is intrinsically slow (catalyst of low activity). For $\Phi_s > 5$ a good approximation for Eq. (11-52) is

$$\eta = \frac{1}{\Phi_s} \tag{11-54}$$

For such large Φ_s intraparticle diffusion has a large effect on the rate. Practically, these conditions mean that diffusion into the pellet is *relatively* slow, so that reaction occurs before the reactant has diffused far into the pellet. In fact, an alternate definition for η is the fraction of the whole surface that is as active as the external surface. If $\eta \to 1$, Eq. (11-43) shows that the rate for the whole pellet is the same as the rate if all the surface were available to reactant at concentration C_s; i.e., the rate at the center is the same as the rate at the outer surface—all the surface is fully effective. In this special case the concentration profile shown in Fig. 11-6 would be horizontal, with $C = C_s$. In contrast, if $\eta \ll 1$, only the surface near the outer periphery of the pellet is effective; the concentration drops from C_s to nearly zero in a narrow region near r_s. In this case the catalyst in the central portion of the pellet is not utilized. Note that such a situation is caused by large pellets, low D_e, or high k_1. The latter factor shows that low effectiveness factors are more likely with a very active catalyst. Thus the more active the catalyst, the more likely it is that intrapellet diffusion resistance will reduce the global rate.

Equations (11-52) and (11-53) provide a method for accounting for intrapellet mass transport for one case, a spherical pellet, and first-order irreversible reaction. The effect of shape on the η-vs.-Φ relationship has been examined by

several investigators.† For a flat plate (slab) of catalyst *sealed from reactants on one side* and all ends,

$$\eta = \frac{\tanh \Phi_L}{\Phi_L} \tag{11-55}$$

$$\Phi_L = L\sqrt{\frac{k_1 \rho_p}{D_e}} \tag{11-56}$$

where L is the thickness of the plate. The curve for Eq. (11-55), as well as flat plate curves for zero and second-order kinetics, are also shown in Fig. 11-8. The first-order curves for spherical and flat-plate geometry show little deviation—less than the error involved in evaluating k_1 and D_e. Hence the shape of the catalyst pellet is not very significant,‡ provided the different definitions of Φ_L and Φ_s are taken into account. For example, suppose the intrinsic rate is second order for a spherical catalyst particle. We may obtain a reasonably accurate η value by using the second-order curve for a plate in Fig. 11-8. However, in using this curve we would take L equal to r_s 3 for evaluating Φ_L. The curve for the flat plate can also be used when both sides of the plate are exposed to reactants, provided L is one-half the plate thickness.

First-order kinetics was chosen in writing Eq. (11-46), so that an analytical solution could be obtained. Numerical solutions for η vs. Φ have been developed for many other forms of rate equations.§ Solutions include those for Langmuir-Hinshelwood equations¶ with denominator terms, as derived in Chap. 9 [e.g., Eq. (9-21)]. To illustrate the extreme effects of reaction, Wheeler†† obtained solutions for zero- and second-order kinetics for a flat plate of catalyst, and these results are also shown in Fig. 11-8. For many catalytic reactions the rate equation is approximately represented by a first-, second-, or intermediate-order kinetics. In these cases the curves for first- and second-order kinetics in Fig. 11-8 define a region within which the effectiveness factor will lie. For unusual situations—for example, when the desorption of a reaction product limits the rate—η values outside of this region may exist. For unusual cases the previous references of Hougen, Schneider, Satterfield, and their colleagues should be consulted. Also,

† R. Aris, *Chem. Eng. Sci.*, 6, 262 (1957); A Wheeler in W. G. Frankenburg, V. I. Komarewsky, and E. K. Rideal (eds.), "Advances in Catalysis," vol. III, Academic Press, Inc., New York, 1951.

‡ The curve for η vs. Φ for a cylinder lies between the curves for the sphere and flat plate in Fig. 11-8. For first-order kinetics, Φ for the cylinder (no axial diffusion) is defined

$$\Phi_c = (r_c/2)\sqrt{k_1 \rho_p / D_e}$$

§ O. A. Hougen and Chu, *Chem. Eng. Sci.*, 17, 167 (1962); P. Schneider and R. A. Mitschka, *Collection Czecho. Chem. Commun.*, 30, 146 (1965), 31, 1205, 3677 (1966); P. Schneider and R. A. Mitschka, *Chem. Eng. Sci.*, 21, 455 (1965).

¶ G. W. Roberts and C. N. Satterfield, *Ind. Eng. Chem., Fund. Quart.*, 4, 288 (1965), 5, 317, 325 (1966).

†† A. Wheeler in W. G. Frankenburg, V. I. Komarewsky, and E. K. Rideal (eds.), "Advances in Catalysis," vol. III, Academic Press, Inc., New York, 1951. The definition of Φ_L for the second-order curve is $L(k_2 C_s \rho_p / D_e)^{1/2}$, where k_2 is the conventional second-order rate constant. For the zero-order case $\Phi_L = (k_0 \rho_p C_s D_e)^{1/2}$.

Aris† has presented a comprehensive mathematical treatment of the effectiveness-factor problem, including the effects of particle shape, multiple reactions, and nonisothermal operation, as well as various types of kinetics. Bischoff‡ has developed a procedure for evaluating η for any form of kinetics by defining a generalized Thiele-type modulus.

The earliest studies of diffusion and reaction in catalysts were by Thiele,§ Damkoehler,¶ and Zeldowitsch.†† Thiele considered the problem from the standpoint of a single cylindrical pore (see Prob. 11-12). Since the catalytic area per unit length of diffusion path does not change in a straight cylindrical pore whose walls are catalytic, the results are of the form of those for a flat plate [Eqs. (11-55) and (11-56)].

Nothing has been said as yet about reversible reactions. For the first-order case the irreversible result can be used, with some modification, for reversible reactions (Example 11-6).

Example 11-6 Derive equations for the effectiveness factor for a first-order reversible reaction $A \rightleftharpoons B$ at isothermal conditions, for a spherical catalyst pellet.

SOLUTION It has been shown [Eqs. (2-62) and (2-64)] that the rate equation for a reversible first-order reaction can be written

$$r = k_R(C - C_{eq}) \tag{A}$$

where C_{eq} is the equilibrium concentration of reactant at the temperature involved, and k_R is related to the forward-rate constant k_1 and the equilibrium constant K by

$$k_R = \frac{k_1(K + 1)}{K} \tag{B}$$

Since Eq. (A) is to be applied to a catalytic reaction, the rate is expressed as g mol/(s)(g catalyst) and k_R has the dimensions cm^3/(s)(g catalyst).

The mass balance of reactant on a spherical shell (see Fig. 11-7) will be the same as Eq. (11-45) except for the reaction term; that is,

$$\left(-4\pi r^2 D_e \frac{dC}{dr}\right)_r - \left(-4\pi r^2 D_e \frac{dC}{dr}\right)_{r+\Delta r} = 4\pi r^2\, \Delta r \rho_p k_R(C - C_{eq})$$

Taking the limit as $\Delta r \to 0$ and replacing C with the variable $C' = C - C_{eq}$,

$$\frac{d^2C'}{dr^2} + \frac{2}{r}\frac{dC'}{dr} - \frac{k_R\rho_p}{D_e}C' = 0 \tag{C}$$

† Rutherford Aris, "The Mathematical Theory of Diffusion and Reaction in Permeable Catalysts," chaps. 3-5, vol. I, Clarendon Press, Oxford, 1975.

‡ K. B. Bischoff, *AIChE J.*, **11**, 351 (1965).

§ E. W. Thiele, *Ind. Eng. Chem.*, **31**, 916 (1939).

¶ G. Damkoehler, *Chem. Eng.*, **3**, 430 (1937).

†† J. B. Zeldowitsch, *Acta Physicochim. U.R.S.S.*, **10**, 583 (1939).

The boundary conditions are

$$\frac{dC'}{dr} = 0 \qquad \text{at } r = 0 \tag{D}$$

$$C' = C_s - C_{eq} = C'_s \qquad \text{at } r = r_s \tag{E}$$

Equations (C) to (E) are the same as Eqs. (11-46) to (11-48), with C' replacing C and k_R replacing k_1. Hence the solution for the effectiveness factor will be identical with Eq. (11-52), but Eq. (11-50) for Φ_s becomes

$$\Phi'_s = \frac{r_s}{3}\sqrt{\frac{k_1(K+1)\rho_p}{KD_e}} \tag{11-57}$$

These results show that the first-order curves in Fig. 11-8 can be used for reversible as well as irreversible reactions, provided k_1 in the definition of Φ_s or Φ_L is replaced by $k_1(K+1)/K$. Since $(K+1)/K$ is greater than unity, Φ will be greater, and η less, for reversible reactions than for irreversible ones.

11-8 The Significance of Intrapellet Diffusion: Evaluation of the Effectiveness Factor

Isothermal effectiveness factors for practical reactions cover a wide range. With normal pellet sizes ($\frac{1}{8}$ to $\frac{1}{2}$ in.) η is 0.7 to 1.0 for intrinsically slow reactions, such as the ammonia synthesis, and of the order of $\eta = 0.1$ for fast reactions, such as some hydrogenations of unsaturated hydrocarbons. Satterfield† and Sherwood‡ have summarized much of the experimental data for effectiveness factors for various reactions, temperatures, and pellet sizes. For reactor design it is important to be able to answer these questions:

1. Should intrapellet diffusion resistance be considered in evaluating the global rate? That is, is η significantly less than unity?
2. If $\eta < 1$, how can η be evaluated from a minimum of experimental data?

We use the results of Sec. 11-7 to formulate answers to these questions.

Suppose that the rate $\mathbf{r}_p$ is measured at a given bulk concentration of reactant. Suppose also that either the external resistance is negligible, or the surface concentration C_s has been evaluated from the bulk value by the methods discussed in Chap. 10. Weisz§ has provided a criterion for deciding, from these measurements and D_e, whether intrapellet diffusion may be disregarded. The basic premise is that if $\Phi_s \leq \frac{1}{3}$, then η is not much less than unity (Fig. 11-8 indicates that η will be

† C. N. Satterfield, "Mass Transfer in Heterogeneous Catalysis," pp. 152-156, Massachusetts Institute of Technology Press, Cambridge, Mass., 1970.

‡ C. N. Satterfield and T. K. Sherwood, "The Role of Diffusion in Catalysis," pp. 72-75, Addison-Wesley Publishing Company, Reading, Mass., 1963.

§ P. B. Weisz, *Z. Phys. Chem.*, **11**, 1 (1957).

greater than 0.9 for $\Phi_s \leq \frac{1}{3}$). Equation (11-50) shows that the criterion may be written

$$r_s \sqrt{\frac{k_1 \rho_P}{D_e}} \leq 1$$

or

$$r_s^2 \frac{k_1 \rho_P}{D_e} \leq 1 \tag{11-58}$$

The unknown rate constant k_1 can be eliminated in favor of the measured rate $\mathbf{r}_P$ from Eq. (11-44), noting that $\eta \to 1.0$. In terms of $\mathbf{r}_P$ Eq. (11-58) becomes

$$r_s^2 \frac{\mathbf{r}_P \rho_P}{C_s D_e} \leq 1 \tag{11-59}$$

The usefulness of Eq. (11-59) stems from the fact that the curves for η vs. Φ for first- and higher-order reactions in Fig. 11-8 would be nearly coincident at $\Phi_s \leq \frac{1}{3}$. Hence Eq. (11-59) is satisfactory as an approximate criterion for most catalytic kinetics, even though it was derived for a first-order case.

Example 11-7 The rate of isomerization of *n*-butane with a silica-alumina catalyst is measured at 5 atm (507 kPa) and 50°C (323 K) in a laboratory reactor with high turbulence in the gas phase surrounding the catalyst pellets. Turbulence ensures that external-diffusion resistances are negligible, so that $C_s = C_b$. Kinetic studies indicate that the rate is first order and reversible. At 50°C the equilibrium conversion is 85%. The effective diffusivity is 0.08 cm²/s at reaction conditions, and the density of the catalyst pellets is 1.0 g/cm³, regardless of size. The measured, global rates when pure *n*-butane surrounds the pellets are as follows:

d_p, in.	1/8	1/4	3/8
$\mathbf{r}_P$, g mol (s)(g catalyst) or kg mol (s)(kg catalyst)	4.85×10^{-4}	4.01×10^{-4}	3.54×10^{-4}

(*a*) To reduce pressure drop in the proposed fixed-bed reactor it is desirable to use the maximum pellet size for which there will be little reduction in the global rate due to intrapellet resistances. The heat of isomerization is low enough that the whole pellet is at 50°C. What is the largest size pellet that may be used? (*b*) Calculate the effectiveness factor for each size.

SOLUTION (*a*) In Example 11-6 the proper definition of Φ_s' for a reversible first-order reaction was shown to be given by Eq. (11-57). From this definition, the criterion for $\eta \to 1$ is

$$\left(\frac{r_s}{3}\right)^2 \frac{k_1(K+1)\rho_P}{K D_e} \leq \left(\frac{1}{3}\right)^2$$

or

$$r_s^2 \frac{k_1(K+1)\rho_P}{K D_e} \leq 1 \tag{A}$$

The rate for the whole pellet (per unit mass of catalyst) for the first-order reversible case is the same as Eq. (11-44), with $k_R(C_s - C_{eq})$ replacing $k_1 C_s$:

$$\mathbf{r}_P = \eta k_R(C_s - C_{eq}) = \eta\left[\frac{k_1(K+1)}{K}\right](C_s - C_{eq}) \qquad (11\text{-}60)$$

Combining Eqs. (A) and (11-60) to eliminate k_1, and noting that $\eta \to 1$, we obtain

$$r_s^2 \frac{\mathbf{r}_P \rho_P}{D_e(C_s - C_{eq})} \leq 1 \qquad (11\text{-}61)$$

Equation (11-61) is the proper criterion to use for reversible reactions in place of Eq. (11-59).

For an equilibrium conversion of 85%,

$$\frac{C_s - C_{eq}}{C_s} = 0.85$$

At 5 atm and 50°C

$$C_s - C_{eq} = 0.85\frac{p}{R_g T} = 0.85\frac{5}{82(323)}$$
$$= 1.60 \times 10^{-4} \text{ g mole/cm}^3 \ (1.60 \times 10^{-1} \text{ kg/mol/m}^3)$$

With numerical values, Eq. (11-61) becomes

$$r_s^2 \mathbf{r}_P \frac{1.0}{0.08(1.60 \times 10^{-4})} = 7.82 \times 10^4 r_s^2 \mathbf{r}_P \leq 1 \qquad (B)$$

For $\frac{1}{8}$-in. pellets, $r_s = \frac{1}{8}(\frac{1}{2})(2.54) = 0.159$ cm $(0.159 \times 10^{-2}$ m). Hence

$$r_s^2 \frac{\mathbf{r}_P \rho_P}{D_e(C_s - C_{eq})} = 7.82 \times 10^4 (0.159)^2 (4.85 \times 10^{-4}) = 0.95$$

For the other two sizes

$$\frac{r_s^2 \mathbf{r}_P \rho_P}{D_e(C_s - C_{eq})} = 3.2 \qquad \tfrac{1}{4}\text{-in. pellets}$$

$$\frac{r_s^2 \mathbf{r}_P \rho_P}{D_e(C_s - C_{eq})} = 6.3 \qquad \tfrac{3}{8}\text{-in. pellets}$$

The $\frac{1}{8}$-in. pellets are the largest for which intrapellet diffusion has a negligible effect on the rate.

(*b*) To calculate η, one relation between Φ_s' and η is obtained from Eq. (11-57) of Example 11-6 and a second is Eq. (11-52), or the Φ_s curve in Fig. 11-8. From Eqs. (11-57) and (11-60) k_1 can be eliminated, giving

$$\Phi_s' = \frac{r_s}{3}\sqrt{\frac{\mathbf{r}_P \rho_P}{\eta D_e(C_s - C_{eq})}} \qquad (11\text{-}62)$$

Table 11-4

d_p, in.	Φ_s'	η
1/8	0.33	0.93
1/4	0.67	0.77
3/8	1.00	0.68

The only unknowns in Eq. (11-62) are η and Φ_s' for a given pellet size. For the $\frac{3}{8}$-in. pellets

$$\Phi_s' = \frac{0.476}{3}\sqrt{\frac{3.54 \times 10^{-4}(1.0)}{0.08(1.60 \times 10^{-4})\eta}} = 0.158\sqrt{\frac{27.6}{\eta}}$$

Simultaneous solution of this expression and Eq. (11-52) yields

$$\Phi_s' = 1.00 \qquad \eta = 0.68$$

Results for the other sizes, obtained the same way, are shown in Table 11-4.

Example 11-7 illustrates one of the problems in scale-up of catalytic reactors. The results showed that for all but $\frac{1}{8}$-in. pellets intrapellet diffusion significantly reduced the global rate of reaction. If this reduction were not considered, erroneous design could result. For example, suppose the laboratory kinetic studies to determine a rate equation were made with $\frac{1}{8}$-in. pellets. Then suppose it was decided to use $\frac{3}{8}$-in. pellets in the commercial reactor to reduce the pressure drop through the bed. If the rate equation were used for the $\frac{3}{8}$-in. pellets without modification, the rate could be erroneously high. At the conditions of part (*b*) of Example 11-7 the correct $\mathbf{r}_P$ would be only 0.68/0.93, or 73% of the rate measured with $\frac{1}{8}$-in. pellets.

With respect to the second question of this section, part (*b*) of Example 11-7 illustrated one method of evaluating η when intrapellet mass transfer is important. In addition to an experimentally determined rate, it was necessary to know the effective diffusivity of the pellet. The need for D_e may be eliminated by making rate measurements for two or more sizes of pellets, provided D_e is the same for all sizes. To show this, note from Eq. (11-44) that the ratio of the rates for two sizes 1 and 2 is

$$\frac{(\mathbf{r}_P)_2}{(\mathbf{r}_P)_1} = \frac{\eta_2}{\eta_1} \tag{11-63}$$

Also, from Eq. (11-50),

$$\frac{(\Phi_s)_2}{(\Phi_s)_1} = \frac{(r_s)_2}{(r_s)_1} \tag{11-64}$$

Furthermore, Eq. (11-52) gives a relation between η and Φ_s which must be satisfied for both pellets. These are the four relations between the four unknowns, η_1, $(\Phi_s)_1$,

η_2, $(\Phi_s)_2$. Solution by trial is easiest. One procedure† is to assume a value of η_2 and calculate η_1 from Eq. (11-63). Determine $(\Phi_s)_1$ from Eq. (11-52); then $(\Phi_s)_2$ can be calculated from Eq. (11-64). Finally, applying Eq. (11-52) for pellet 2 gives a revised value of η_2. The calculations are continued until the initial and calculated values of η_2 agree. This method is illustrated in Example 11-8 where data including the effect of external mass transport are analyzed. The method is not valid for large Φ_s, for then Eq. (11-52) reduces to Eq. (11-54), and combination with Eqs. (11-63) and (11-64) shows that the rate is inversely proportional to r_s *for all sizes.*

If one of the pellets for which $\mathbf{r}_P$ is measured is very small (e.g., powder form), η equals 1.0 for that size. Then the ratio of Eq. (11-43) for the small pellet, $(\mathbf{r}_P)_1$, and a larger size pellet, $(\mathbf{r}_P)_2$, gives, for any reaction order,

$$\frac{(\mathbf{r}_P)_2}{(\mathbf{r}_P)_1} = \frac{\eta_2 f(C_s)}{1.0 f(C_s)}$$

or

$$\eta_2 = \frac{(\mathbf{r}_P)_2}{(\mathbf{r}_P)_1} \tag{11-65}$$

Hence the effectiveness factor for a given pellet can be obtained by measuring the rate for the pellet and for a small particle size of the same catalyst at the same concentration of reactant.

The rate measurement for the small particles determines the rate of the chemical reaction at the catalyst site, i.e., without intrapellet-diffusion resistance. Then the rate constant k can be calculated directly. Thus it is not necessary that the measurements for the small particles and the pellet be at the same concentration of reactant, as required by Eq. (11-65). Consider an irreversible first-order reaction. From Eq. (11-44),

$$k_1 = \frac{(\mathbf{r}_P)_1}{(C_s)_1} \tag{11-66}$$

since $\eta_1 = 1.0$. Using this value of k_1 in Eq. (11-44), applied to the pellet, we have

$$\eta_2 = \frac{(\mathbf{r}_P)_2}{(C_s)_2 k_1} = \frac{(\mathbf{r}_P/C_s)_2}{(\mathbf{r}_P/C_s)_1} \tag{11-67}$$

Example 11-8 To illustrate the analysis of laboratory-reactor data to account for the combined effects of external and internal mass transfer, consider the following information.‡

A differential, packed-bed, catalytic reactor (ID = 0.95 cm) is used to study hydrogenation of α-methyl styrene to cumene. Liquid styrene containing only dissolved hydrogen is pumped through a short bed of Pd/Al_2O_3 catalyst particles. The concentration of H_2 in the flowing liquid stream is

† C. N. Satterfield and T. K. Sherwood, loc. cit.

‡ M. Herskowitz, Ph.D. Thesis, University of California, Davis, 1978

approximately constant throughout the reactor and equal to 2.6×10^{-6} g mol/cm^3. The reactor operates at a constant temperature of 40.6°C and at steady state. Catalyst and reactor-bed properties are:

Catalyst = 0.2 wt% Pd on Al_2O_3 (granular)
Particle density, $\rho_p = 1.53$ g/cm^3
Bed void fraction, $\varepsilon_p = 0.48$
Particle porosity $\varepsilon_p = 0.50$

Table 11-5 gives the reaction rate, **r** (determined by measuring the production of cumene), as a function of liquid flow rate, Q, for two sizes (d_p = equivalent spherical diameter) of catalyst particles. Both sizes were taken from the same batch of catalyst. At these conditions the reaction rate is first order with respect to hydrogen.

From the data given calculate effectiveness factors and the effective diffusivity for hydrogen in the liquid-filled pores of the catalyst particles.

SOLUTION In this study of the reaction,

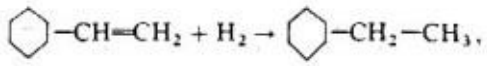

there is no gas phase, and the pores of the catalyst are filled with liquid. Even though the particle sizes are small, the low diffusivity in liquids may mean that intraparticle diffusion retards the rate. Also, the increase in reaction rate with liquid flow rate shown in Table 11-5 indicates that external mass transfer retards the rate. Under these conditions the global rate is given by Eq. (11-44) and also by the external mass transfer expression, Eq. (10-1). Equating these rate equations:

$$r_p = \eta k_1 (C_{H_2})_s = k_m a_m (C_b - C_s)_{H_2} \qquad \text{(A)}$$

Table 11-5 Global rate data for the hydrogenation of α-methyl styrene

Q cm^3/s	$r \times 10^6$ g mol (g catalyst)(s)	
	$d_p = 0.054$ cm	$d_p = 0.162$ cm
2.5	.....	0.65
3.0	1.49	
5.0	1.56	0.72
8.0	1.66	0.80
10.0	1.70	0.82
11.5	.....	0.85
12.5	1.80	
15.0	1.90	0.95
25.0	1.94	1.02
30.0	.....	1.01

where k_m is the mass transfer coefficient and a_m is the mass transfer area per unit mass of catalyst. The last equality can be solved for C_s and then substituted in the first equality to obtain the rate in terms of the bulk liquid concentration. Doing this, and omitting the H_2 subscript, gives

$$\mathbf{r} = \frac{C_b}{1/k_1\eta + 1/k_m a_m}$$

or

$$\frac{C_b}{\mathbf{r}} = \frac{1}{k_1\eta} + \frac{1}{k_m a_m} \tag{B}$$

Experimental data are available for $\mathbf{r}$ vs. Q. Since $k\eta$ is not a function of liquid flow rate and $k_m a_m$ is, Eq. (B) can be used to separate and evaluate $k\eta$ and $k_m a_m$. Then the values for $k\eta$ for the two particle sizes permit determining k and η separately by using Eqs. (11-63) and (11-64).

An alternate procedure would be to use the correlation of Eq. (10-10) with Eq. (10-9) to evaluate $k_m a_m$. Then $k\eta$ would be obtained from Eq. (B). It is probably more accurate to use the experimental data for the effect of Q, rather than the correlation, and we will follow this procedure.

Combination of Eqs. (10-9) and (10-10) to eliminate j_D indicates that $k_m a_m$ is proportional to $(d_p G/\mu)^b$, or Q^b, at constant d_p. Then Eq. (B) becomes

$$\frac{C_b}{\mathbf{r}} = \frac{1}{k_1\eta} + A\frac{1}{Q^b} \tag{C}$$

where A is a constant for data at different Q and the same catalyst particle size. Equation (C) shows that a graph of known values of C_b/r vs. Q^{-b} should be a straight line with an intercept, at $Q^{-b} = 0$, equal to $1/k_1\eta$. The power b is given as 0.407 in the correlation of Eq. (10-10). However, we can establish b by trial, noting the value which leads to the best straight line. This b would supposedly account for the characteristics of the particular bed (uniformity of packing, etc.) not accounted for in Eq. (10-10).

Figure 11-9 shows that with $b = 0.3$ the data establish reasonably good straight lines.† The intercepts are

$$(k_1\eta_1)^{-1} = 0.77 \quad \text{for} \quad (d_p)_1 = 0.054 \text{ cm} \tag{D}$$

$$(k_1\eta_2)^{-1} = 1.32 \quad \text{for} \quad (d_p)_2 = 0.162 \text{ cm} \tag{E}$$

Since k_1 is the same for both particle sizes, the ratio of the intercepts gives

$$\frac{\eta_1}{\eta_2} = \frac{(k_1\eta_2)^{-1}}{(k_1\eta_1)^{-1}} = \frac{1.32}{0.77} = 1.71$$

† A range of b values (from 0.25 to 0.45) give good straight lines for all of which the intercepts are about the same. Since there are sufficient data points, a linear mean square fit of the data might be a logical way to establish $k_1\eta$.

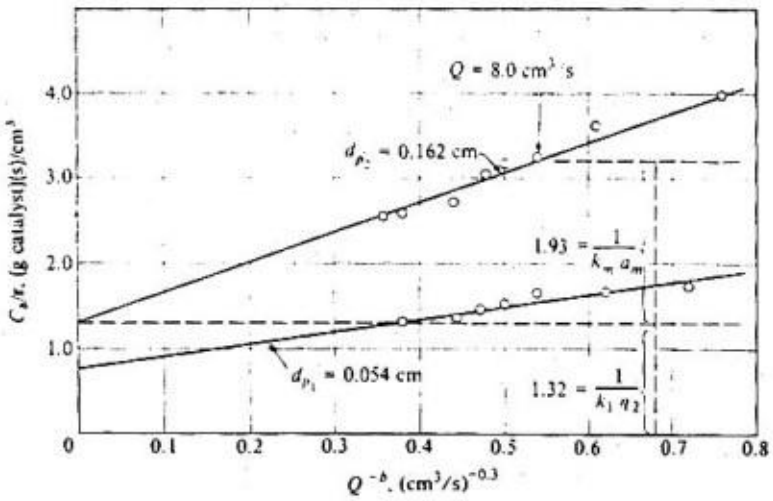

Figure 11-9 Effect of external mass transfer on global rate for hydrogenation of α-methyl styrene.

This equation is analogous to Eq. (11-63). Equation (11-64) provides the second relation between η_1, η_2, $(\phi_s)_1$ and $(\phi_s)_2$:

$$\frac{(\Phi_s)_1}{(\Phi_s)_2} = \frac{(d_p)_2}{(d_p)_1} = \frac{0.054}{0.162} = 0.333$$

The other two relations (one for each particle size) are provided by Eq. (11-52) or by the curve for spherical particles in Fig. 11-8. Solving by trial

$$\eta_1 = 0.88 \qquad (\Phi_s)_1 = 0.58$$
$$\eta_2 = 0.51 \qquad (\Phi_s)_2 = 1.63$$

Then from Eq. (C)

$$\frac{1}{k_1(0.88)} = 0.77$$

and

$$k_1 = 1.5 \text{ cm}^3/(\text{g})(\text{s})$$

Now the diffusivity can be found from the definition of Φ_s. Thus, from Eq. (11-50) for d_{p_1}

$$(\Phi_s)_1 = 0.58 = \frac{0.054/2}{3}\left[\frac{1.5(1.53)}{D_e}\right]^{1/2}$$
$$D_e = 5.5 \times 10^{-4} \text{ cm}^2/\text{s}$$

This diffusivity is relatively high for liquids (see Sec. 11-3) but is typical of values for dissolved hydrogen. Note that for the larger particles the effect of both external and internal transport was significant for this relatively fast reaction. For example, at $Q = 8.0\ \text{cm}^3/\text{s}$ from Fig. 11-9, the values of the terms in Eq. (B) are, for $(d_p)_2 = 0.162$ cm

$$\frac{2.6 \times 10^{-6}}{0.80 \times 10^{-6}} = 3.25 = \frac{1}{1.5(0.51)} + 1.93$$

$$= 1.32 + 1.93$$

At these conditions the resistance to external mass transfer (1.93) is greater than the combined resistance (1.32) of reaction and intraparticle diffusion. Also, the η_2 of 0.51 means that the effect of intraparticle diffusion was to reduce the intrinsic rate by 50%.

11-9 Experimental and Calculated Effectiveness Factors

When the rate is measured for a catalyst pellet and for small particles, and the diffusivity is also measured or predicted, it is possible to obtain both an experimental and a calculated result for η. For example, for a first-order reaction Eq. (11-67) gives η_{exp} directly. Then the rate measured for the small particles can be used in Eq. (11-66) to obtain k_1. Provided D_e is known, Φ can be evaluated from Eq. (11-50) for a spherical pellet or from Eq. (11-56) for a flat plate of catalyst. Then η_{calc} is obtained from the proper curve in Fig. 11-7. Comparison of the experimental and calculated values is an overall measure of the accuracy of the rate data, effective diffusivity, and the assumption that the intrinsic rate of reaction (or catalyst activity) is the same for the pellet and the small particles.
Example 11-9 illustrates the calculations and results for a flat-pellet of NiO catalyst, on an alumina carrier, used for the ortho-para-hydrogen conversion.

Example 11-9† The pellet reactor is shown in Fig. 11-10. The reaction gases were exposed to one face of the cylindrical disk (1 in. in diameter and $\frac{1}{4}$ in. in depth), while the other face and the cylindrical surface were sealed. Vigorous turbulence near the exposed face ensured uniform composition in the gas region and eliminated external diffusion resistance. The reaction

$$o\text{-}H_2 \rightleftharpoons p\text{-}H_2$$

has a very low heat of reaction, and the whole reactor was enclosed in a liquid nitrogen bath. Thus isothermal conditions obtain at -196°C.

Rates were measured at -196°C and 1 atm pressure for pellets of three densities. The rate of reaction was also measured for the catalyst in the form of 60-micron (average size) particles. With this small size, $\Phi \ll 1$ so that $\eta = 1.0$. The rate data and pellet properties are given in Table 11-6.

† This example is taken from the data of M. R. Rao, N. Wakao, and J. M. Smith, *Ind. Eng. Chem.*, 3, 127 (1964).

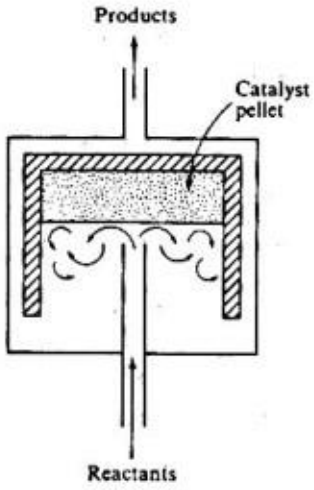

Figure 11-10 Reactor for a single, flat-plate catalyst pellet.

Table 11-6 Catalyst and rate data for ortho-hydrogen conversion on NiO/Al_2O_3

Catalyst particles
$d_p = 60$ microns
$S_g = 278\ m^2/g$
$V_g = 0.44\ cm^3/g$
$\rho_S = 2.63\ g/cm^3$
$\rho_p = 2.24\ g/cm^3$
$\hat{a}_M = 29$ Å (from integration of pore-volume distribution)
$k_g = 0.688\ cm^3/(s)(g)$, calculated from the measured rate $(r_p)_1$, for the small particles ($\eta = 1.0$) using Eq. (A) of Example 11-6.

Catalyst pellets			
ρ_p, g/cm³	ϵ_M	Macropore radius $\hat{a}_M$, Å	$(r_p)_2/(C_s - C_{eq})$ cm³/(s)(g)
1.09	0.48	2,100	0.186
1.33	0.37	1,690	0.129
1.58	0.33	1,270	0.109

Note: The physical-property data were obtained from pore-size distribution and surface-area measurements, as described in Chap. 8.

SOLUTION Equation (11-67) is for an irreversible reaction, and so it cannot be used to calculate η_{exp} for the ortho-hydrogen reaction. The proper equation is obtained by applying Eq. (11-60) to the pellet. Solving for η gives

$$\eta_{exp} = \frac{(r_P)_2}{k_R(C_s - C_{eq})_2}$$

From this equation and the data given in Table 11-6, η_{exp} can be immediately evaluated. The results are:

ρ_P	η_{exp}
1.09	$\frac{0.186}{0.688} = 0.27$
1.33	$\frac{0.129}{0.688} = 0.19$
1.58	$\frac{0.109}{0.688} = 0.16$

To obtain η_{calc} we must estimate the effective diffusivity. Since the macropores are much larger than the micropores (see $\bar{a}_M$ and $\bar{a}_\mu$ in Table 11-6), it is safe to assume that diffusion is predominantly through the macropores. Then, according to the random-pore model [Eqs. (11-27) and (11-28)],

$$D_e = \varepsilon_M^2 \frac{1}{1/\mathscr{D}_{H_2} + 1/(\bar{\mathscr{D}}_K)_{H_2}} \tag{A}$$

For hydrogen at $-196°C$ and 1 atm, $\mathscr{D}_{H_2} = 0.14\ cm^2/s$. Using Eq. (11-17) and the $\bar{a}_M$ values from Table 11-5, we obtain:

ρ_P	1.09	1.33	1.58
$(\bar{\mathscr{D}}_K)_{H_2}$, cm^2/s	1.28	1.03	0.77

From Eq. (A), the effective diffusivity is, for $\rho_P = 1.09$,

$$D_e = 0.48^2 \frac{1}{1/0.14 + 1/1.28} = 0.029\ cm^2/s$$

The results for the other pellet densities are given in the second column of Table 11-7. The Thiele-type modulus is calculated from Eq. (11-56), modified for a reversible reaction by substituting k_R for k_1:

$$\Phi_L' = L\sqrt{\frac{k_R \rho_P}{D_e}} = \frac{1}{4}(2.54)\sqrt{\frac{0.688(1.09)}{0.029}} = 3.2$$

From the first-order Φ_L-vs.-η curve in Fig. 11-8 for a flat plate, $\eta_{calc} = 0.30$. The results for all three pellets are given in the last columns of the table.

Table 11-7

ρ_p	D_e, cm²/s	Φ_L	η_{calc}	η_{exp}
1.09	0.029	3.2	0.30	0.27
1.33	0.017	4.6	0.21	0.19
1.58	0.013	5.7	0.17	0.16

The calculated and experimental effectiveness factors agreed well with each other in Example 11-9. Note that the calculated η required the rate for the small particles as the only experimental data. Hence the method offers an attractive procedure for predicting the rate for any size of pellet. However, there are data for other catalysts and reactions which suggest less favorable agreement. Results for the same reaction with a catalyst of NiO supported on silica gel showed good coincidence between η_{exp} and η_{calc}.† With Vycor as a carrier the agreement for effectiveness factors is reasonably good, even though calculated (by the random-pore model) and experimentally measured D_e were in poor accord‡ Relatively large deviations in D_e cause small differences in η. Otani and Smith§ applied the method to the reaction

$$CO + \tfrac{1}{2}O_2 \rightarrow CO_2$$

using spherical catalyst pellets of NiO on Al_2O_3. The calculated η were 50 to 100% higher than the experimental results, depending on the temperature. The reasons for the large deviation were obscure, but a decrease in catalyst activity may have been caused by plugging of some of the pores in the particles when the pellets were formed. Such results emphasize that the method of predicting η depends on assuming that the intrinsic rate of reaction is the same for the surface in the small particles as for the surface in the pellet. Another possible error in the method is the variation in effective diffusivity within a pellet. It has been found¶ that D_e can vary with position near the surface of a pellet, presumably because of skin effects caused by nonuniform stresses in the pelleting process.

11-10 The Effect of Intrapellet Mass Transfer on Observed Kinetics

In Sec. 10-1 we saw that neglecting external resistances could lead to misleading conclusions about reaction order and activation energy. Similar errors may occur when intrapellet mass transfer is neglected. Consider the situation where $\Phi_s > 5$. In this region intrapellet transport has a strong effect on the rate: Fig. 11-8 shows

† M. R. Rao and J. M. Smith, *AIChE J.*, **9**, 445 (1963).
‡ M. R. Rao and J. M. Smith, *AIChE J.*, **10**, 293 (1964).
§ Seiya Otani and J. M. Smith, *J. Catalysis*, **5**, 332 (1966).
¶ C. N. Satterfield and S. K. Saraf, *Ind. Eng. Chem., Fund. Quart.*, **4**, 451 (1965).

that η is less than about 0.2. From Eqs. (11-54) and (11-50) for a first-order reaction

$$\eta = \frac{3}{r_s}\sqrt{\frac{D_e}{k_1 \rho_P}}$$

and for second-order kinetics

$$\eta = \frac{3}{r_s}\sqrt{\frac{D_e}{k_2 \rho_P C_s}}$$

Using these expressions for η in the equations for the rates for the whole pellet [for example, Eq. (11-44)], we obtain

$$\mathbf{r}_P = \frac{3C_s}{r_s}\sqrt{\frac{D_e k_1}{\rho_P}} \qquad \text{first order}$$

$$\mathbf{r}_P = \frac{3C_s^{3/2}}{r_s}\sqrt{\frac{D_e k_2}{\rho_P}} \qquad \text{second order}$$

If the rate constants are expressed as Arrhenius functions of temperature, $k = \mathbf{A}e^{-E/R_g T}$, then

$$\mathbf{r}_P = \frac{3\mathbf{A}_1^{1/2} C_s}{r_s}\left(\frac{D_e}{\rho_P}\right)^{1/2} e^{-E/2R_g T} \qquad \text{first order} \qquad (11\text{-}68)$$

$$\mathbf{r}_P = \frac{3\mathbf{A}_2^{1/2} C_s^{3/2}}{r_s}\left(\frac{D_e}{\rho_P}\right)^{1/2} e^{-E/2R_g T} \qquad \text{second order} \qquad (11\text{-}69)$$

These equations give the correct influence of concentration and temperature when intrapellet diffusion is important.

Now suppose intrapellet resistance is neglected. The rate for a first-order reaction would be correlated in terms of the apparent activation energy E_a by the expression

$$\mathbf{r}_P = \mathbf{A}_1 e^{-E_a/R_g T} C_s \qquad (11\text{-}70)$$

Comparison of Eqs. (11-70) and (11-68) indicates that the apparent activation energy determined from Eq. (11-70) would be one-half the true value, E. The measured rate, when plotted in Arrhenius coordinates, would appear as in Fig. 11-11. At low enough temperatures the data would determine a line with a slope equal to $-E/R_g$, because η would approach unity. However, at high enough temperatures intrapellet diffusion would be important; Eq. (11-68) would be applicable, and a line with a slope of $-\frac{1}{2}E/R_g$ would result. These conclusions would be the same regardless of the reaction order.

Equations (11-68) and (11-69) show that the rate $\mathbf{r}_P$ (recall that it is for the whole pellet, but per unit mass of catalyst) is inversely proportional to pellet size r_s. If intrapellet diffusion is neglected, the rate is independent of pellet size, as illustrated by Eq. (11-70).

If diffusion in the pores is of the Knudsen type, D_e is independent of pressure, and therefore of concentration. Then Eq. (11-68) indicates that first-order kinetics would be observed, even though intrapellet diffusion is important. However, a

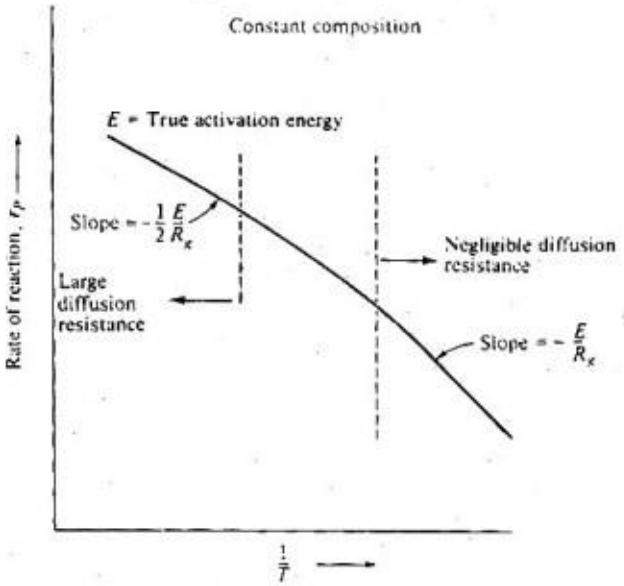

Figure 11-11 Effect of intrapellet diffusion on apparent activation energy.

second-order reaction would appear to be of order $\frac{3}{2}$. If bulk diffusion were involved, $D_e \approx 1/p$. Hence when concentration is varied by changing the pressure, a first-order reaction would appear to be of order $\frac{1}{2}$. Similarly, Eq. (11-69) shows that a second-order reaction would appear to be first order.

These effects have been observed in many instances. In particular, the flattening of the line on an Arrhenius plot (as in Fig. 11-11) is frequently found when heterogeneous reactions are studied over a wide temperature range (see Example 11-10).

Example 11-10 In Example 11-8 the reaction was first order. Now we examine the same type of problem for nonlinear kinetics using experimental global rate data for the catalytic oxidation of dilute solutions of acetic acid with dissolved oxygen. The data were given in Example 9-3 and the results for the small particle sizes were analyzed there to determine an equation for the intrinsic rate. The result was Eq. (B) of Example 9-3. Our objective here is to use the data for the largest particles to establish the importance of intraparticle diffusion in the liquid-filled pores.

(*a*) Using the data given in Example 9-3 calculate effectiveness factors at each temperature for the 0.18 cm (diameter) particles.

(*b*) Estimate the intraparticle diffusivity and tortuosity factor at 280°C. The molecular diffusivities of oxygen and of acetic acid in water at 68 atm and 280°C are estimated to be 2.0×10^{-4} cm^2/s and 1.2×10^{-4} cm^2/s, respectively.

(*c*) Calculate an activation energy for the reaction and also an apparent value, E_a, from the global rate data given for the 0.18 cm particles.

SOLUTION

(*a*) The rate data for various temperatures (given in the third table of the problem statement for Example 9-3) are for constant concentrations of both oxygen and acetic acid. Also, the effectiveness factor for 0.054 cm particles is 1.0, as explained in Example 9-3. Hence, Eq. (11-65) is applicable for evaluating the effectiveness factors. At 260°C ($10^3\ T = 1.876$),

$$(\eta)_{d_p=0.18} = \frac{(r_p)_{d_p=0.18}}{(r_p)_{d_p=0.054}} = \frac{1.40}{2.00} = 0.70$$

For all the temperatures (using rate values from the table) the results are:

t, °C	280	270	260	250
$(\eta)_{d_p=0.18}$	0.59	0.64	0.70	0.79

(*b*) Since the intrinsic rate equation is available, and we know η, the effective diffusivity can be calculated. If the kinetics were first order, this would be simple. From η at a particular temperature we evaluate Φ_s from Fig. 11-8. Then from Eq. (11-50), using the known k and particle size (r_s), D_e could be calculated. For the nonlinear kinetics of Eq. (B) of Example 9-3 another approach must be used. An exact method would be to write a differential mass balance like Eq. (11-46) but using Eq. (B) for the intrinsic rate. This balance could be integrated numerically to find $C = f(r)$ and then to evaluate an effectiveness factor, as is done in Sec. 11-7. Alternately, we could search the literature† to see if such a solution for the kinetics of Eq. (B) was already available. Let us use a third approach (already mentioned), that of defining a generalized Thiele modulus suitable for any type of kinetics.‡ According to this method η is still given by Eq. (11-52), but the generalized Thiele modulus is, for spherical pellets and for oxygen,

$$\Phi_s = \frac{r_s}{3}(\mathbf{r}_{O_2})_s \left[2 \int_0^{(C_{O_2})_s} \mathbf{r}_{O_2} D_e \, dC_{O_2} \right]^{-1/2} \qquad \text{(A)}$$

where $(\mathbf{r}_{O_2})_s$ is the rate of disappearance of oxygen evaluated at the surface concentration (which is equal to the bulk value in this case).

The quantity $\mathbf{r}_{O_2}$ is equal to $\mathbf{r}_{CO_2}$ so that Eq. (B) of Example 9-3 gives $\mathbf{r}_{O_2}$. To carry out the integration indicated in Eq. (A), C_{HA} in Eq. (B) must be expressed in terms of C_{O_2}. This is done by noting that stoichiometry

† For example, in G. W. Roberts and C. N. Satterfield, *Ind. Eng. Chem. Fundam.*, 4, 288 (1965); 5, 317 (1966).

‡ K. B. Bischoff, *AIChE J.*, 11, 351 (1965).

requires that the mass transfer rate of oxygen be twice that of acetic acid. Hence,

$$(D_e)_{O_2}\frac{dC_{O_2}}{dr} = 2(D_e)_{HA}\frac{dC_{HA}}{dr} \tag{B}$$

Integrating from the outer surface to any intraparticle radius r yields

$$(D_e)_{O_2}[(C_{O_2})_s - C_{O_2}] = 2(D_e)_{HA}[(C_{HA})_s - C_{HA}]$$

or

$$C_{HA} = (C_{HA})_s + \frac{1}{2}\left(\frac{D_{O_2}}{D_{HA}}\right)[C_{O_2} - (C_{O_2})_s] \tag{C}$$

Equation (C) gives C_{HA} in terms of C_{O_2} and the known surface concentrations. The effective diffusivity ratio, $(D_e)_{O_2}/(D_e)_{HA}$, is equal to the molecular diffusivity ratio by Eq. (11-26), since the porosity ε_p and tortuosity factor δ are properties of the geometry of the catalyst particle and should be the same for oxygen and acetic acid.

Equation (C) can be substituted for C_{HA} in Eq. (B) of Example 9-3 to obtain an expression for r_{O_2} with C_{O_2} as the only variable. With this expression the term in brackets in Eq. (A) can be integrated directly to yield

$$\left[2(D_e)_{O_2}\int_0^{(C_{O_2})_s} r_{O_2}\,dC_{O_2}\right] = 2(D_e)_{O_2}k_A B\int_0^{(C_{O_2})_s}\frac{C_{O_2}^{3/2}\,dC_{O_2}}{1 + k_B(A + BC_{O_2})} - 2(D_e)_{O_2}k_A A\int_0^{(C_{O_2})_s}\frac{C_{O_2}^{1/2}\,dC_{O_2}}{1 + k_B(A + BC_{O_2})} \tag{D}$$

where

$$A = (C_{HA})_s - \frac{1}{2}\left(\frac{D_{O_2}}{D_{HA}}\right)(C_{O_2})_s \tag{E}$$

$$B = \frac{1}{2}\frac{D_{O_2}}{D_{HA}} \tag{F}$$

Now all quantities on the right-hand side of Eq. (A) are known except D_e. Surface concentrations for oxygen and for acetic acid are equal to their bulk values. The molecular diffusivities are known at 280°C, as are k_A and k_B in the intrinsic rate equation. The rate at the *surface* is, from Eq. (B) of Example 9-3,

$$(r_{O_2})_s = (r_{CO_2})_s = \frac{k_A(C_{O_2})_s^{1/2}(C_{HA})_s}{1 + k_B(C_{HA})_s} \tag{G}$$

A solution procedure is: first evaluate Φ_s from Eq. (11-52) at 280°C using the η values found in part (*b*). Then taking $r_s = d_p/2 = 0.18$ cm, find the value of $(D_e)_{O_2}$ from the right-hand side of Eq. (A) which agrees with this value of Φ_s. With $\eta = 0.59$, $\Phi_s = 1.25$ and, by trial, $(D_e)_{O_2} = 2 \times 10^{-5}$ cm^2/s.

Finally, the tortuosity factor is obtained from $(D_e)_{O_2}$ using Eq. (11-26).

$$\delta = \frac{\varepsilon_p D_{O_2}}{(D_e)_{O_2}} = \frac{0.55(2 \times 10^{-4})}{2 \times 10^{-5}} = 5.5$$

In contrast to the first-order curve in Fig. 11-8, the effectiveness factor for nonlinear kinetics will depend upon the surface concentrations. For example, for reactor design the objective is to determine η and a global rate for known intrinsic kinetics. In this case we would use Eq. (A) to calculate Φ_s, and then evaluate η from Eq. (11-52). The result would depend upon surface concentrations through Eq. (D) and $(\mathbf{r}_{O_2})_s$. This means that the effectiveness factor would vary with location in an integral reactor.

(*c*) Suppose that the effect of temperature on the intrinsic rate, given by Eq. (B) and the values of k_A and k_B in Example 9-3, can be represented by the Arrhenius equation

$$\mathbf{r}_{CO_2} = Ae^{-E/R_gT} f(C_{O_2}, C_{HA}) \qquad \text{(H)}$$

Then the slope of a plot of $\mathbf{r}_{CO_2}$ vs. $1/T$ at constant composition is equal to $-E/R_g$. To obtain the correct activation energy for the chemical reaction, the rate values must exclude mass transport effects. This was shown to be true in Example 9-3 for the 0.038 and 0.054 cm particles. Such a plot is shown in Fig. 11-12 for the data in the third table of Example 9-3, which

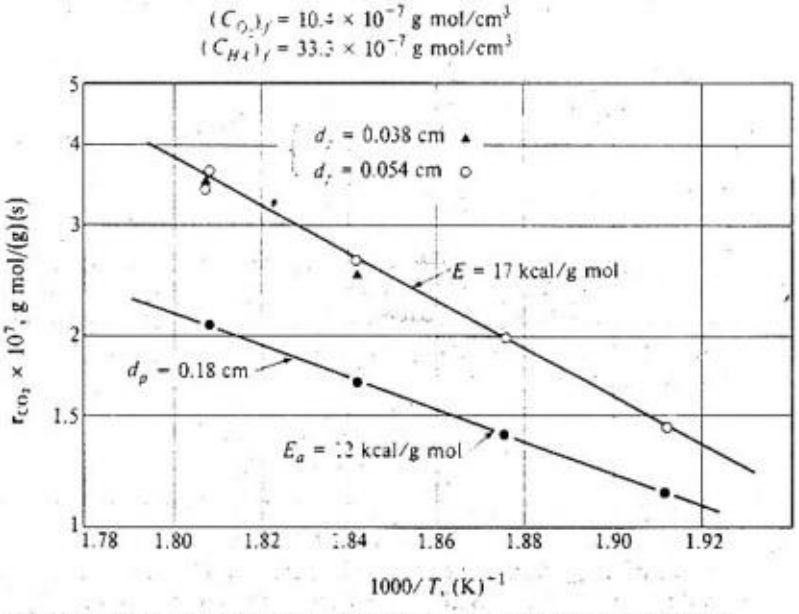

Figure 11-12 Effects of temperature and particle size on oxidation rate of acetic acid.

sary because Eqs. (11-46) and (11-72) are coupled through the nonlinear dependence of k_1 on temperature; $k_1 = Ae^{-E/R_gT}$. Nevertheless, the similarity of the nonreaction terms in the two differential equations does permit an analytical relation between concentration of reactant and temperature at any point in the pellet. Thus eliminating $k_1 \rho_p C$ from the two equations yields

$$D_e\left(\frac{d^2C}{dr^2} + \frac{2}{r}\frac{dC}{dr}\right) = \frac{k_e}{\Delta H}\left(\frac{d^2T}{dr^2} - \frac{2}{r}\frac{dT}{dr}\right)$$

or

$$D_e \frac{d}{dr}\left(r^2 \frac{dC}{dr}\right) = \frac{k_e}{\Delta H}\frac{d}{dr}\left(r^2 \frac{dT}{dr}\right) \tag{11-75}$$

If this equation is integrated once, using Eqs. (11-47) and (11-73) for the boundary conditions, and then integrated a second time, using Eqs. (11-48) and (11-74),

$$T - T_s = \frac{(\Delta H)D_e}{k_e}(C - C_s) \tag{11-76}$$

This result, originally derived by Damkoehler,† is not restricted to first-order kinetics, but is valid for any form of rate expression, since the rate term was eliminated in forming Eq. (11-75). The maximum temperature rise in a pellet would occur when the reactant has been consumed by the time it diffuses to the center. Applying Eq. (11-76) for $C = 0$ gives

$$(T_c - T_s)_{\max} = -\frac{(\Delta H)D_e}{k_e} C_s \tag{11-77}$$

Equation (11-77) shows that the maximum temperature rise depends on the heat of reaction, transport properties of the pellet, and the surface concentration of reactant. It permits a simple method of estimating whether intrapellet temperature differences are significant (see Example 11-11).

Let us return to the nonisothermal effectiveness factor. Weisz and Hicks solved Eqs. (11-46) and (11-72) numerically‡ to determine the concentration profile within the pellet. Then η was obtained from Eq. (11-51), which is not limited to isothermal conditions, provided k_1 is evaluated at the surface temperature. The results expressed η as a function of three dimensionless parameters:

1. The Thiele-type modulus,

$$3(\Phi_s)_s = r_s\sqrt{\frac{(k_1)_s \rho_p}{D_e}} \tag{11-78}$$

Note that Φ_s is evaluated at the surface temperature; that is, $(k_1)_s$ in Eq. (11-78) is the rate constant at T_s.

† G. Damkoehler, *Z. Phys. Chem.*, **A193**, 16 (1943).

‡ P. B. Weisz and J. S. Hicks, *Chem. Eng. Sci.*, **17**, 265 (1962). Actually, Eq. (11-76) permitted expression of k_1 as a function of concentration rather than of temperature ($k_1 = Ae^{-E/R_gT}$). This uncoupled Eqs. (11-46) and (11-72), so that only Eq. (11-46) needed to be solved.

2. The Arrhenius number,

$$\gamma = \frac{E}{R_g T_s} \tag{11-79}$$

3. A heat-of-reaction parameter,

$$\beta = \frac{(-\Delta H) D_e C_s}{k_e T_s} \tag{11-80}$$

Figure 11-13 shows η as a function of $(\Phi_s)_s$ and β for $\gamma = 20$, which is in the middle of the practical range of γ. Weisz and Hicks give similar figures for $\gamma = 10$, 30, and 40. The curve for $\beta = 0$ corresponds to isothermal operation ($\Delta H = 0$) and is identical with the curve for a spherical pellet in Fig. 11-8.

For an exothermic reaction (positive β) the temperature rises going into the pellet. The increase in rate of reaction accompanying the temperature rise can more than offset the decrease in rate due to drop in reactant concentration. Then η values are greater than unity. While $\eta > 1$ increases the rate per pellet, and therefore the production per unit mass of catalyst, there may also be some disadvantages. With large η there will be a large increase in temperature toward the center of the pellet, resulting in sintering and catalyst deactivation. The desired product may be subject to further reaction to unwanted product, or undesirable side reactions may occur. If these reactions have higher activation energies than the desired reaction, the rise in temperature would reduce selectivity.

For an endothermic reaction there is a decrease in temperature and rate into the pellet. Hence η is always less than unity. Since the rate decreases with drop in temperature, the effect of heat-transfer resistance is diminished. Therefore the curves for various β are closer together for the endothermic case. In fact, the decrease in rate going into the pellet for endothermic reactions means that mass

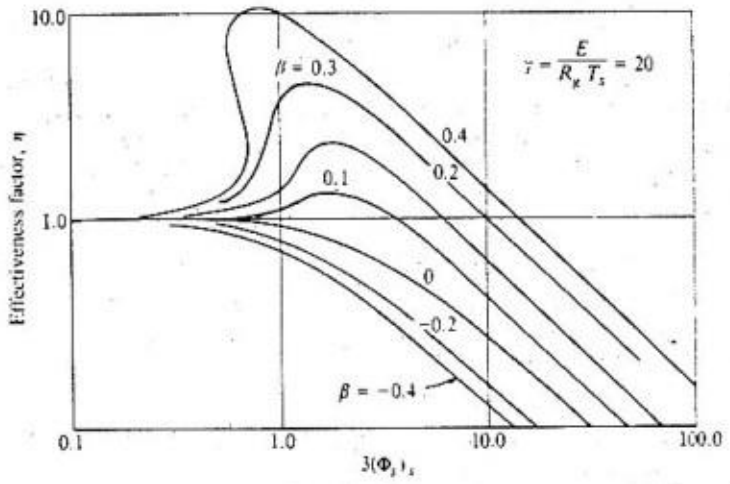

Figure 11-13 Nonisothermal effectiveness factors for first-order reactions in spherical catalyst pellets.

transfer is of little importance. It has been shown† that in many endothermic cases it is satisfactory to use a *thermal* effectiveness factor. Such thermal η neglects intrapellet mass transport; that is, η is obtained by solution of Eq. (11-72), taking $C = C_s$ (see Prob. 11-14).

Figure 11-13 indicates that for $\beta > 0.3$ and $3(\Phi_s)_s < 1.0$, up to three values of η exist for a single set of γ, $3(\Phi_s)_s$, and β. Such behavior can be explained by noting that the equality of heat evolved due to reaction and heat transferred by conduction in the pellet (such equality must exist for steady-state operation) can occur with different temperature profiles. Thus the solution giving the highest η for a given β curve in Fig. 11-13 would correspond to a steep temperature profile in the pellet; physical processes dominate the rate for the whole pellet. The solution for the lowest η, which is near unity, corresponds to small temperature gradients in the pellet; the rate is controlled by the chemical-reaction step. The intermediate η is identified as a metastable state, similar to the metastable conditions described in Sec. 10-4.

Carberry‡ has shown that for $(\Phi_s)_s > 2.5$ the η-vs.-$(\Phi_s)_s$ relationship could be characterized approximately by the single parameter $\beta\gamma$, rather than by γ and β separately. For example, for a first-order irreversible reaction he found

$$\eta = \frac{1}{(\Phi_s)_s} e^{\beta\gamma/5} \qquad \text{for } (\Phi_s)_s > 2.5 \tag{11-81}$$

where

$$\beta\gamma = \frac{(-\Delta H) D_e C_s}{k_e T_s} \frac{E}{R_g T_s} \tag{11-82}$$

Carberry also obtained results for a second-order rate equation.

In Sec. 11-8, Eq. (11-59) was developed as a criterion for deciding if intrapellet mass transport had a significant effect on the rate. Weisz and Hicks§ have extended the analysis to the problem of combined mass and energy transport. For a first-order irreversible reaction the criterion may be expressed as

$$\Theta = r_s^2 \frac{\mathbf{r}_p \rho_p}{C_s D_e} e^{\gamma\beta/(1+\beta)} \leq 1 \tag{11-83}$$

where γ and β are defined by Eqs. (11-79) and (11-80). When $\beta = 0$ (isothermal conditions) this criterion reduces to Eq. (11-59). As in that equation, $\mathbf{r}_p$ is the measured rate. Thus the significance of intrapellet gradients can be evaluated from measurable or known properties. If $\Theta \leq 1$, the nonisothermal effectiveness factor will be near unity, so that intrapellet gradients can be neglected.

11-12 Experimental Nonisothermal Effectiveness Factors

The magnitude of intrapellet temperature differences and nonisothermal η are illustrated by the following examples, based on experimental measurements for specific systems.

† J. A. Maymo, R. E. Cunningham, and J. M. Smith, *Ind. Eng. Chem., Fund Quart.*, 5, 280 (1966).
‡ J. J. Carberry, *AIChE J.*, 7, 350 (1961).

Example 11-11 Rate data for the reaction $H_2 + \frac{1}{2}O_2 \rightarrow H_2O$ have been measured† for single catalyst pellets (1.86-cm diameter) of platinum on Al_2O_3. Catalyst properties, k_e, D_e, and center and surface temperatures were also evaluated. The rate was obtained in a stirred-tank reactor in which the pellet was surrounded by well-mixed reaction gases. In one run the data were as follows:

Gas temperature $t_g = 90°C$
Average surface temperature $t_s = 101°C$
Pellet-center temperature $t_c = 148°C$
Density of catalyst particles in pellet‡ = 0.0602 g catalyst/cm^3
Mole fraction oxygen at pellet surface = 0.0527
Effective diffusivity of pellet = 0.166 cm^2/s
Effective thermal conductivity = 6.2×10^{-4} cal/(s)(cm)(°C)
Pellet rate of reaction, $\mathbf{r}_p = 2.49 \times 10^{-5}$ g mol O_2/(g catalyst)(s)
Total pressure $p_t = 1$ atm

Rate data were also obtained for the small (80 to 250 mesh) particles from which the pellets were prepared. The results, expressed as the rate of oxygen consumption, g mol/(g catalyst)(s), were correlated by

$$\mathbf{r}_{part} = 0.327 p_{O_2}^{0.804} e^{-5.230/R_g T}$$

where p_{O_2} is in atmospheres. Do internal concentration and temperature gradients have a significant effect on the pellet rate? Estimate the maximum temperature difference, $T_c - T_s$.

SOLUTION Equation (11-83) will be satisfactory as a criterion, since the Φ_s-vs.-η curves for a first-order reaction will be nearly the same as those for 0.8 order:

$$(C_{O_2})_s = \frac{(p_{O_2})_s}{R_g T} = \frac{1(0.0527)}{82(101 + 273)} = 1.72 \times 10^{-6} \text{ mole/cm}^3$$

$$r_s^2 \frac{\mathbf{r}_p \rho_p}{C_s D_e} = \left(\frac{1.86}{2}\right)^2 \frac{2.49 \times 10^{-5}(0.0602)}{1.72 \times 10^{-6}(0.166)} = 4.4$$

From Eqs. (11-79) and (11-80),

$$\gamma = \frac{5{,}230}{2(374)} = 7.0$$

$$\beta = \frac{115{,}400(0.166)(1.72 \times 10^{-6})}{6.2 \times 10^{-4}(374)} = 0.14$$

† J. A. Maymo and J. M. Smith, *AIChE J.*, 12, 845 (1966).

‡ The spherical pellet was prepared by compressing a mixture of inert Al_2O_3 particles and Al_2O_3 particles containing 0.005 wt % platinum. The ratio of active to total particles was 0.1. The density of the pellet was 0.602 g/cm^3, so that the density of catalyst particles in the pellet was 0.0602.

Note that the heat of reaction per mole of oxygen is $-57{,}700(2) = -115{,}400$ cal/g mol.

Introducing these results in Eq. (11-83) gives

$$\Theta = (4.4)e^{7(0.14)\,1.14} = 4.4(2.36) = 10.4$$

Since the value of Θ far exceeds unity, intrapellet resistances do affect the rate.

Equation (11-77) gives the maximum value for $T_c - T_s$.

$$T_c - T_s = -\frac{(-115{,}400)(0.166)}{6.2 \times 10^{-4}}(1.72 \times 10^{-6}) = 52°C$$

The observed temperatures gives $148 - 101 = 47°C$. Comparison between the maximum and observed $T_c - T_s$ suggests that the oxygen is nearly all consumed when it reaches the center of the pellet. Hence the rate also will vary with radial position due to the drop in reactant (O_2) concentration.

This preliminary analysis suggests that both intrapellet temperature and concentration gradients will significantly affect the rate. Since the reaction is exothermic, the two factors have opposite effects on the rate per pellet. The dominant effect can be ascertained by calculating the resultant effectiveness factor.

Example 11-12 From the experimental data given in Example 11-11 evaluate the effectiveness factor for the catalyst pellet. Also predict η, using the results of Weisz and Hicks.†

SOLUTION The *particles* for which rates were measured are small enough that η is unity. Hence an experimental effectiveness factor can be obtained from Eq. (11-65). This equation was derived for isothermal operation but will be applicable for nonisothermal conditions as long as the two rates are evaluated at the same surface temperature as well as reactant concentration. Applying Eq. (11-65)

$$\eta_{exp} = \frac{\mathbf{r}_p(\text{at } T_s, C_s)}{\mathbf{r}_{part}(\text{at } T_s, C_s)}$$

The rate for the particles at T_s and C_s is obtainable from the correlation of particle rates given in Example 11-10:

$$\mathbf{r}_{part} = 0.327(0.0527^{0.804})e^{-5.230/(374)} = 2.77 \times 10^{-5} \text{ g mol } O_2/(\text{g catalyst})$$

Then

$$\eta_{exp} = \frac{2.49 \times 10^{-5}}{2.77 \times 10^{-5}} = 0.9$$

To calculate η we first obtain $3(\Phi_s)_s$, using Eq. (11-78). The reaction is not first order, and so $(k_1)_s$ is not known. However, it may be replaced by its equivalent, $\mathbf{r}/C$, where $\mathbf{r}$ is the rate of the chemical step, that is, the rate

† P. B. Weisz and J. S. Hicks, *Chem. Eng. Sci.*, 17, 265 (1962).

uninfluenced by intrapellet resistances. This is the rate measured for the small catalyst particles, 2.77×10^{-5} g mol/(g catalyst)(s). Hence

$$3(\Phi_s)_s = r_s\sqrt{\frac{r_{part}\rho_p}{C_s D_e}} = \frac{1.86}{2}\sqrt{\frac{2.77 \times 10^{-5}(0.0602)}{1.72 \times 10^{-6}(0.166)}} = 2.20$$

With this value for $3(\Phi_s)_s$, and $\gamma = 7.0$ and $\beta = 0.14$, a calculated η can be found from the Weisz and Hicks charts [similar to Fig. (11-13)]. The value is difficult to estimate from the available charts, but is approximately

$$\eta_{calc} = 0.94$$

A more accurate η can be obtained by solving equations such as (11-46) and (11-72) but avoiding the first-order restriction. This can be done by replacing $k_1 C$ in the reaction term of each equation with the more correct relationship $kp_{O_2}^{0.804}$. Maymo did this, solving the differential equations numerically by means of a high-speed digital computer. The calculated η for $3(\Phi_s)_s = 2.20$, $\gamma = 7.0$, and $\beta = 0.14$ is $\eta_{calc} = 0.96$. The calculated η for a first-order reaction agrees somewhat better with the experimental result. Probably this is not significant, because the calculated values rest on the assumption that the intrinsic rate is the same for the particles as for the pellets. There is evidence† to indicate that when the particles are made into pellets there is a slight reduction in intrinsic rate owing to partial blocking of the micropores in the particles. Regardless of the reasons for the small deviation (7%), the agreement between calculated and experimental η is quite adequate, particularly in view of the variety of independent data (D_e, k_c, rates, etc.) that are required to calculate the effectiveness factor.

Since η is less than unity, the effect of the concentration gradient is more important than the effect of the temperature gradient in this instance.

The significance of the thermal effect on the pellet rate is established primarily by β and secondarily by γ. For example, Otani and Smith‡ studied the reaction $CO + \frac{1}{2}O_2 \rightarrow CO_2$, making measurements similar to the $H_2 + O_2$ reaction, but at temperatures from 250 to 370°C. Here β was of the order of 0.05 and $\gamma = 9.7$. Intrapellet temperature gradients were much lower than in Example 11-11: the largest measured value for $T_c - T_s$ was 7°C. In contrast, hydrogenation reactions have large heats of reaction; D_e is relatively high for hydrogen, and often T_s is low. All these factors tend to increase β. Cunningham et al.§ found β to be of the order of 0.5 (and γ about 25) for the hydrogenation of ethylene, and thermal effects were large. Similarly, in the work of Prater* for the dehydrogenation of cyclohexane, β and γ were sufficient to reduce η significantly.

† J. A. Maymo and J. M. Smith, *AIChE J.*, 12, 845 (1966).

‡ S. Otani and J. M. Smith, *J. Catalysis*, 5, 332 (1966).

§ R. A. Cunningham, J. J. Carberry, and J. M. Smith, *AIChE J.*, 11, 636 (1965).

* C. D. Prater, *Chem. Eng. Sci.*, 8, 284 (1958), as analyzed in C. N. Satterfield and T. K. Sherwood "The Role of Diffusion in Catalysis," p. 90, Addison-Wesley Publishing Company, Reading, Mass, 1963.

Increasing reactant concentration increases β and η. When the partial pressure of oxygen was increased to 0.11 atm in the $H_2 + O_2$ reaction, with other conditions approximately the same as in Example 11-11, β became 0.34, and the experimental η was 1.10. At these conditions $T_c - T_s$ increased to $219 - 118 = 101°C$.

EFFECT OF INTERNAL TRANSPORT ON SELECTIVITY AND POISONING

In many catalytic systems, multiple reactions occur, so that selectivity becomes important. In Sec. 2-11 point and overall selectivities were evaluated for homogeneous, well-mixed systems of parallel and consecutive reactions. In Sec. 10-5 we found that external diffusion and heat-transfer resistances in consecutive reactions affected the selectivity. Here we shall examine the influence of intrapellet resistances. Systems with first-order kinetics at isothermal conditions are analyzed analytically in Sec. 11-13 for parallel and consecutive reactions. Results for other kinetics, or for nonisothermal conditions, can be developed in a similar way but require numerical solution.†

11-13 Selectivities for Porous Catalysts

The selectivity at a location in a fluid-solid catalytic reactor is equal to the ratio of the global rates at that point. The combined effect of both external and internal diffusion resistance can be displayed easily for parallel irreversible, first-order reactions. We shall do this first and then consider how internal resistance influences the selectivity for other reaction sequences.

Consider two parallel reactions of the independent form

$$1.\quad A \xrightarrow{k_1} B + C \qquad \text{(desired)}$$

$$2.\quad R \xrightarrow{k_2} S + W$$

where $k_1 > k_2$.

An example might be the dehydrogenation of mixed feed of propane and *n*-butane, where the desired catalyst is selective for the *n*-butane dehydrogenation. Suppose that the temperature is constant and that both external and internal diffusion resistances affect the rate. At steady state, the rate (for the pellet, expressed per unit mass of catalyst) may be written in terms of either Eq. (10-1) or Eq. (11-44),

$$r_p = k_m a_m (C_b - C_s) \tag{11-84}$$

or

$$r_p = \eta k_1 C_s \tag{11-85}$$

† Selectivity for Langmuir-Hinshelwood kinetics of the form of Eqs. (9-21) and (9-27), have been evaluated for isothermal conditions by G. Roberts and C. N. Satterfield [*Ind. Eng. Chem., Fund. Quart.*, 4, 288 (1965)] and J. Hutchings and J. J. Carberry [*AIChE J.*, 12, 20 (1966)].

where a_m is the external area for mass transfer per unit mass of catalyst. The surface concentration can be eliminated between (11-84) and (11-85) to give

$$\mathbf{r}_P = \frac{1}{1/k_m a_m + 1/\eta k_1} C_b \tag{11-86}$$

This expression is equivalent to Eq. (B) developed in Example 11-8 and expresses the combined effect of external and internal mass-transport resistances. Note that the reduction in rate due to internal diffusion (through η) is combined with the rate constant k for the chemical step, while the external effect is separate. If the external resistance is negligible, then $k_m a_m \gg \eta k_1$. If internal transport is insignificant, then $\eta \to 1$. If both conditions are satisfied, the rate is determined solely by the chemical step; that is, Eq. (11-85) reduces to $\mathbf{r}_P = k_1 C_b$.

The selectivity of product B with respect to product S for a pellet in the reactor is obtained by applying Eq. (11-86) to the two reactions; thus the pellet selectivity S_P is

$$S_P = \frac{(\mathbf{r}_P)_1}{(\mathbf{r}_P)_2} = \frac{[1/(k_m)_B a_m + 1/\eta_2 k_2](C_A)_b}{[1/(k_m)_A a_m + 1/\eta_1 k_1](C_B)_b} \tag{11-87}$$

If there were neither external nor internal resistances, the pellet selectivity would be

$$S_P = \frac{k_1 (C_A)_b}{k_2 (C_B)_b} \tag{11-88}$$

Since $(k_m)_B$ and $(k_m)_A$ will not differ greatly, comparison of Eqs. (11-87) and (11-88) shows that external-diffusion resistance reduces the selectivity. The same conclusion was reached in Sec. 10-5 for parallel independent reactions (see Eq. (10-29c). To evaluate qualitatively the effect of internal diffusion note that k_1 is presumably greater than k_2 (B is the desired product). Since Φ increases, and, therefore, η decreases as k increases (see Fig. 11-8), η_1 will be less than η_2. Then Eq. (11-87) indicates that internal diffusion also decreases the selectivity.

Equation (11-86) shows that the external effect on the rate can always be treated as a separate, additive resistance. From here on we shall focus on internal effects, using Eq. (11-85) for the global rate and taking bulk and surface concentrations to be equal. The internal problem can be expressed analytically if we are satisfied with examining the extreme case of large intrapellet resistance characterized by $\Phi_s \geq 5$ ($\eta \leq 0.2$) where Eq. (11-54) is valid. Then Eq. (11-85) becomes

$$\mathbf{r}_P = \frac{1}{\Phi_s} k_1 C_b = \frac{3}{r_s} \sqrt{\frac{k_1 D_e}{\rho_P}} C_b \tag{11-89}$$

If Eq. (11-89) is applied to the stated, independent parallel reactions, the selectivity is

$$S_P = \frac{(\mathbf{r}_P)_1}{(\mathbf{r}_P)_2} = \frac{\sqrt{\overline{k_1 (D_A)_e}}(C_A)_b}{\sqrt{\overline{k_2 (D_B)_e}}(C_B)_b} \tag{11-90}$$

Neglecting differences in diffusivities of A and R, we have

$$S_p = \left(\frac{k_1}{k_2}\right)^{1/2} \frac{(C_A)_b}{(C_R)_b} \tag{11-91}$$

Comparing Eqs. (11-88) and (11-91) shows that the effect of *strong* intrapellet diffusion resistance is to reduce the selectivity to the square root of its intrinsic value.

Wheeler† characterized the *independent parallel* reactions $A \rightarrow B$ and $R \rightarrow S$ as *type I selectivity*. *Type II selectivity* refers to *parallel* reactions with a common reactant:

$$1.\quad A \xrightarrow{k_1} B$$

$$2.\quad A \xrightarrow{k_2} C$$

An example would be the dehydration of ethanol to ethylene and its dehydrogenation to acetaldehyde. If both reactions are first order and irreversible, selectivity is unaffected by internal mass transport; the ratio of the rates of reactions 1 and 2 is k_1/k_2 at any position within the pellet. This same conclusion applied for external transport [Sec. 10-5, Eq. (10-29)]. Equation (11-89) cannot be applied separately to the two reactions because of the common reactant A. The development of the effectiveness-factor function would require writing a differential equation analogous to Eq. (11-45) for the *total* consumption of A by both reactions. Hence k in Eq. (11-89) would be $k_1 + k_2$ and $\mathbf{r}_p$ would be $(\mathbf{r}_p)_1 + (\mathbf{r}_p)_2$. Such a development would shed no light on selectivity.

If the kinetics of the two reactions are different, diffusion has an effect on selectivity. Suppose reaction 2 is second order in A and reaction 1 first order. The reduction in concentration of A due to diffusion resistance would lower the rate of reaction 2 more than that of reaction 1. For this case the selectivity of B would be improved by diffusion resistance.

Type III selectivity applies to *successive* reactions of the form

$$A \xrightarrow{k_1} B \xrightarrow{k_3} D$$

where B is the desired product. Examples include successive oxidations, successive hydrogenations, and other sequences, such as dehydrogenation of butylenes to butadiene, followed by polymerization of the butadiene formed. In Chap. 2, Eq. (2-87) was developed for the intrinsic selectivity of B with respect to A,‡ that is, the point selectivity determined by the kinetics of the reactions,

$$S = \frac{\text{net rate of production of } B}{\text{rate of disappearance of } A} = \frac{dC_B}{-dC_A} = 1 - \frac{k_3}{k_1}\frac{C_B}{C_A} \tag{11-92}$$

† The treatment in this section follows in part that developed by A. Wheeler in W. G. Frankenburg, V. I. Komarewsky, and E. K. Rideal (eds.), "Advances in Catalysis," vol. III, p. 313, Academic Press, Inc., New York, 1951; and P. P. Weisz and C. D. Prater in "Advances in Catalysis," vol. VII, Academic Press, Inc., New York, 1954.

‡ In Sec. 10-5 the same successive reactions were analyzed. There the selectivity of B with respect to final product D was considered, rather than the selectivity with respect total disappearance of reactant A.

Equation (11-92) is also applicable for the whole catalyst pellet when diffusion resistance is negligible and gives the selectivity at any location within the pellet. The selectivity will vary with position in the pellet as C_B/C_A changes. Diffusion resistance causes C_A to decrease going from the outer surface toward the center of the pellet. Since B is formed within the pellet and must diffuse outward in order to enter the bulk stream, C_B increases toward the pellet center. Equation (11-92) shows qualitatively that these variations in C_A and C_B both act to reduce the global, or pellet, selectivity for B.

A quantitative interpretation can also be developed. For first-order reactions the variation of C_A with radial position in a spherical pellet is given by Eq. (11-49). The concentration profile for B can be obtained in a similar manner by writing a differential mass balance for B. The expression will be like Eq. (11-45), except that the term on the right must represent the *net* disappearance of B; that is, it must account for the conversion of B to D and the production of B from A. Wheeler† solved such a differential equation to obtain $C_B = f(r)$. The solution, combined with Eq. (11-49) for C_A, can be used to obtain the selectivity of B with respect to A as a function of radial position. Integrating across the radius gives the selectivity for the whole pellet. For strong diffusion resistance ($\eta \leq 0.2$) and equal effective diffusivities the result is

$$S_P = \frac{(r_P)_B}{-(r_P)_A} = \frac{(k_1/k_3)^{1/2}}{1 + (k_1/k_3)^{1/2}} - \left(\frac{k_3}{k_1}\right)^{1/2} \frac{(C_B)_b}{(C_A)_b} \tag{11-93}$$

Comparison of Eqs. (11-92) and (11-93) demonstrates that the selectivity is significantly reduced when diffusion resistances are large. The magnitude of the reduction depends on $(C_B/C_A)_b$, which, if external-diffusion resistance is neglected, is equal to C_B/C_A at any position in the reactor. At the entrance to a *reactor* $(C_B/C_A)_b$ is a minimum. If no B is present in the feed, $C_B = 0$ at this point. From Eq. (11-92) the selectivity is 1.0. Equation (11-93) shows that strong diffusion resistance reduces this to

$$S_P = \frac{(k_1/k_3)^{1/2}}{1 + (k_1/k_3)^{1/2}} \tag{11-94}$$

The reduction is most severe for small values of k_1/k_3.

Suppose the pellet selectivity for B is observed to be low in the $A \rightarrow B \rightarrow D$ series of reactions, and diffusion resistance is significant. Either preparing the catalyst with larger pores or reducing the pellet size may improve the selectivity. However, these changes would be most effective if they increased η from a low value to near unity. The changes would be wholly ineffective if η remained ≤ 0.2, since Eq. (11-93) is valid for all η below 0.2. The first change would probably reduce the capacity of a fixed mass, or volume, of catalyst, since the pore surface available for reaction would decrease as pore radius increased. The second change would increase the pressure drop in a fixed-bed reactor.

† A. Wheeler in W. G. Frankenburg, V. I. Komarewsky, and E. K. Rideal (eds.), "Advances in Catalysis," vol. III, Academic Press, Inc., New York, 1951.

Example 11-13 An ethylene stream is fed to a polymerization reactor in which the catalyst is poisoned by acetylene. The ethylene is prepared by catalytically dehydrogenating ethane. Hence it is important that the dehydrogenation catalyst be selective for dehydrogenating C_2H_6 rather than C_2H_4. The first-order reactions are

$$\underset{(A)}{C_2H_6} \xrightarrow{k_1} \underset{(B)}{C_2H_4} \xrightarrow{k_3} \underset{(D)}{C_2H_2}$$

For one catalyst $k_1/k_3 = 16$. It is suspected that intrapellet diffusion strongly retards both dehydrogenations. Estimate the potential improvement in selectivity if diffusion resistance could be eliminated. Make the estimate for a concentration ratio $(C_B/C_A)_b = 1.0$. Neglect differences in D_e between ethane and ethylene.

SOLUTION Equation (11-93) is applicable for the *diffusion-limited* situation. The pellet selectivity for ethylene formation with respect to ethane disappearance is

$$S_P = \frac{16^{1/2}}{1 + 16^{1/2}} - \frac{1}{16^{1/2}}(1) = 0.55$$

If diffusion resistance is eliminated, Eq. (11-92) gives the point as well as the pellet selectivity

$$S_P = 1 - \tfrac{1}{16}(1) = 0.94$$

These selectivities give the ratio of rates of formation of ethylene and total disappearance of ethane (ethylene plus acetylene). If we start with pure C_2H_6, a mass balance requires that the rate of formation of acetylene with respect to disappearance of ethane be $1 - S_P$. Hence eliminating diffusion resistance reduces the rate of formation of undesirable C_2H_2 from 0.45 to 0.06.

The discussion has been limited to selectivities which exist at one conversion (set of concentrations) in a reactor. Wheeler has extended the development to show cumulative selectivities that would exist at any level of conversion in the reactor effluent.

We have seen that when intrapellet temperature gradients exist the rate per pellet (or η) cannot be expressed analytically. Hence selectivities for nonisothermal conditions must be evaluated numerically. Examples are available for several forms of rate equations.†

† John Beek, *AIChE J.*, 7, 337 (1961); John Hutchings and J. J. Carberry, *AIChE J.*, 12, 20 (1966).

11-14 Rates for Poisoned Porous Catalysts

As mentioned in Chap. 8, the rates of fluid-solid catalytic reactions are frequently reduced by poisoning. It is of interest to know how the reduction in rate varies with the extent of catalytic surface which has been poisoned and with on-stream time. Experimental data show that the rate may drop linearly with the fraction of surface poisoned, or it may fall much more rapidly. The second form of behavior may be caused by selective adsorption of the poisoning substance on those catalyst sites which are active for the main reaction. Such adsorption on a relatively small part of the total catalyst would cause a large reduction in rate. An alternate explanation is possible if the main reaction occurs primarily on the outer part of the catalyst pellet (low effectiveness factor) and the poison is also adsorbed primarily in this region. Then a relatively small part of the total surface will be deactivated by poison, but this small part is where the main reaction occurs.

As Wheeler† has shown, the interaction of intrapellet diffusion on the rate of the main and poisoning reactions can lead to a variety of relations between activity and extent of poisoning. We examine some of these here as a further illustration of the effect of intrapellet mass transfer upon the rate of catalytic reactions. It is assumed that the activity of the unpoisoned catalytic surface is the same throughout the pellet and that the main reaction is first order.

The discussion will be for *parallel* and independent poisoning such as caused by deposition of an impurity in the feed stream. Poisoning also commonly occurs by a *successive* reaction sequence. Thus, an intermediate may be the desired product, but reaction continues to end products which are deposited on the catalytic sites. Poisoning by carbon deposition in refinery (e.g., cracking) and petrochemical (e.g., dehydrogenation, etc.) processing are examples. Quantitative treatment and reviews are available‡§ for the reduction in rate due to successive (series) poisoning processes. Also, the treatment here will be for the extremes of uniform distribution of poison or of pore-mouth poisoning, both at isothermal conditions. Examples of more general analysis encompassing the regions in between these extremes are available.¶ Nonisothermal poisoning has also been investigated.¶ ††

Uniform distribution of poison Suppose the rate of the adsorption (or reaction) process which poisons the catalytic site is slow with respect to intrapellet diffusion. Then the surface will be deactivated uniformly through the pellet. If α is the fraction of the surface so poisoned, the rate constant for the *main* reaction will become $k_1(1 - \alpha)$. The rate per pellet, according to Eq. (11-44), is

$$r_p = \eta k_1(1 - \alpha)C_s \tag{11-95}$$

Consider first the case where the diffusion resistance for the main reaction

† A. Wheeler in W. G. Frankenburg, V. I. Komarewsky, and E. K. Rideal (eds.), "Advances in Catalysis," vol. III, p. 307, Academic Press, Inc., New York, 1951.

‡ Shinobu Masamune and J. M. Smith, *AIChE J.*, **12**, 384 (1966).

§ J. B. Butt, "Catalyst Deactivation," *Adv. Chem. Ser.*, vol. 109, p. 259 (1972).

¶ M. Sagara, S. Masamune, and J. M. Smith, *AIChE J.*, **13**, 1226 (1967).

†† E. K. T. Kam and Ronald Hughes, *AIChE J.*, **25**, 359 (1979).

also is low; that is, consider a slow main reaction. Then $\eta \to 1$, and Eq. (11-95) shows that the rate drops linearly with α ($F = 1 - \alpha$). At the other extreme of large intrapellet resistance ($\Phi_s > 5$), $\eta = 1/\Phi_s$, and Eq. (11-95) becomes

$$r_P = \frac{3}{r_s}\sqrt{\frac{D_e}{k_1(1-\alpha)\rho_P}}\,k_1(1-\alpha)C_s$$
$$= \frac{3}{r_s}\sqrt{\frac{D_e}{\rho_P}k_1(1-\alpha)}\,C_s \qquad (11\text{-}96)$$

Hence the effect of poisoning on the rate of the main reaction is proportional to $\sqrt{1-\alpha}$; that is, it is less than a linear effect. This situation, corresponding to a slow poisoning reaction and a fast (large Φ_s) main reaction, was termed *antiselective poisoning* by Wheeler.

The two cases are shown in Fig. 11-14 by curves *A* and *B*, where the ratio *F* of poisoned to unpoisoned rate is plotted against α. Note that the ratio is the quotient of Eq. (11-95) evaluated at any α and at $\alpha = 0$. Thus for curve *B*, from Eq. (11-96),

$$F = \frac{(3/r_s)\sqrt{D_e k_1(1-\alpha)/\rho_P}\,C_s}{(3/r_s)\sqrt{D_e k_1/\rho_P}\,C_s} = \sqrt{1-\alpha} \qquad (11\text{-}97)$$

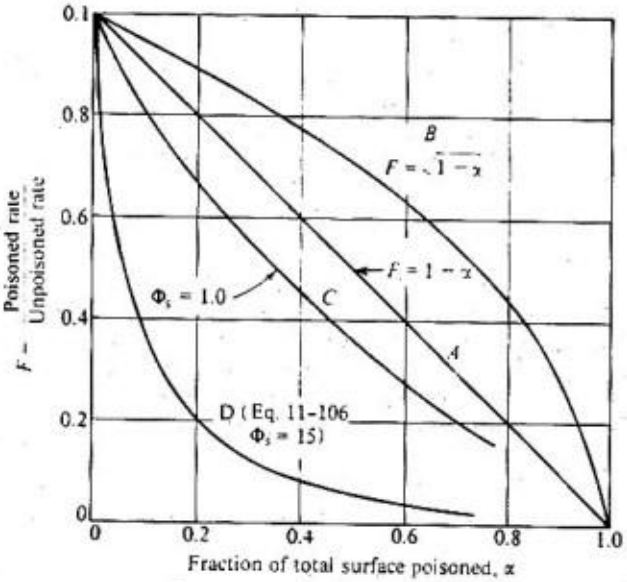

A - Uniform poisoning and slow main reaction $\eta \to 1$
B - Uniform poisoning and fast main reaction $\eta \leq 0.2$
C - Pore-mouth poisoning and slow main reaction $\Phi_s = 1.0$
D - Pore-mouth poisoning and fast main reaction $\Phi_s = 15$

Figure 11-14 Intrapellet diffusion and poisoning in catalytic reactions.

For intermediate cases of diffusion resistance for the main reaction, the curves would fall between A and B in the figure.

Pore-mouth (shell) poisoning If the adsorption (or reaction) causing poisoning is very fast, the outer part of a catalyst pellet will be completely deactivated, while the central portion retains its unpoisoned activity. An example is sulfur poisoning of a platinum-on-Al_2O_3 catalyst, where the sulfur-containing molecules diffuse only a short distance into the pellet before they are adsorbed on the platinum surface. In this type of poisoning a layer of poisoned catalyst will start to grow at the outer surface and will continue to increase in thickness with time† until all the pellet is deactivated. In the extreme case the boundary between the deactivated and active catalyst will remain sharply defined during the deactivation process. This type of poisoning, described by the *progressive shell model*, will be discussed in Chap. 14 in connection with noncatalytic reactions.

The effect of pore-mouth poisoning can be obtained by equating the rate of diffusion through the outer, deactivated layer to the rate of reaction on the inner fully active part of the pellet. Figure 11-15 depicts a spherical catalyst pellet at a *time* when the radius of the unpoisoned central portion is r_c, corresponding to a thickness of completely poisoned catalyst $r_s - r_c$. Consider a first-order reaction where the concentration of reactant at the outer surface is C_s. The rate of diffusion into one pellet will be

$$\mathrm{r} = D_e 4\pi r^2 \frac{dC}{dr} \tag{11-98}$$

This equation is applicable between r_s and r_c. Integrating‡ to express the rate in terms of the concentrations C_s and C_c (at $r = r_c$) gives

$$\mathrm{r} = \frac{4\pi D_e r_s r_c}{r_s - r_c}(C_s - C_c) \tag{11-99}$$

This diffusion rate is equal to the rate of reaction in the inner core, or

$$\mathrm{r} = \frac{4\pi D_e r_s r_c}{r_s - r_c}(C_s - C_c) = m_p \eta k_1 C_c \tag{11-100}$$

where m_p is the mass of the active core of the pellet. The second equality in Eq. (11-100) may be solved for C_c and the result inserted into Eq. (11-99). Taking $m_p = \frac{4}{3}\pi r_c^3 \rho_p$ and dividing by $\frac{4}{3}\pi r_s^3 \rho_p$ to give the rate for the whole pellet, but on a unit mass basis, gives

$$\mathrm{r}_p = \frac{\mathrm{r}}{\frac{4}{3}\pi r_s^3 \rho_p} = \frac{k_1 C_s}{r_s^3 \eta r_c^3 - (k_1 \rho_p r_s^2 / 3D_e)[(r_s - r_c)/r_c]} \tag{11-101}$$

† For example, suppose that the poison is brought into contact with the catalyst pellet as a contaminant in the reactant stream flowing steadily in the reactor. Then the amount of poisoning material available is directly proportional to time.

‡ It is assumed here that the thickness of the poisoned layer is not changing in the time required for diffusion. Then r can be regarded as a constant during this short time interval. Such a pseudo-steady state is discussed in Chap. 14.

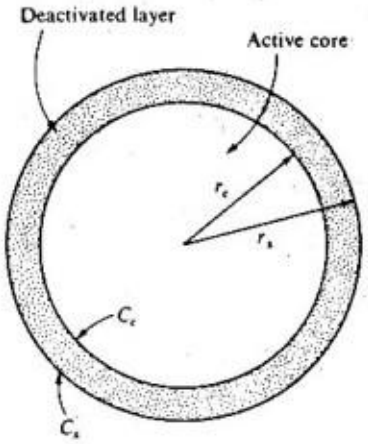

Figure 11-15 Shell model of catalyst poisoning.

The fraction of the total surface unpoisoned is

$$1 - \alpha = \frac{\frac{4}{3}\pi r_c^3 \rho_p S_g}{\frac{4}{3}\pi r_s^3 \rho_p S_g} = \frac{r_c^3}{r_s^3} \tag{11-102}$$

Using this relation for r_c/r_s in Eq. (11-101), the rate in terms of α becomes

$$\mathbf{r}_p = \frac{k_1 C_s}{1 \eta(1-\alpha) + 3\Phi_s^2[1-(1-\alpha)^{1/3}]/(1-\alpha)^{1/3}} \tag{11-103}$$

where Eq. (11-50) has been used to introduce Φ_s. If there is no poisoning, then $\alpha = 0$, and Eq. (11-103) reduces to $\mathbf{r}_p = \eta k_1 C_s$ [i.e., Eq. (11-44)]. Hence the ratio of poisoned and unpoisoned rates is

$$F = \frac{1}{1.(1-\alpha) + 3\eta(\Phi_s)^2[1-(1-\alpha)^{1/3}]/(1-\alpha)^{1/3}} \tag{11-104}$$

Again consider two extremes of the main reaction. If its intrinsic rate is very slow, diffusion resistance in the inner core of active catalyst will be negligible and $\eta \to 1$. At these conditions Φ_s will also be low, but not as small as would be expected. This is because η is a function of $\Phi_c = (r_c/3)\sqrt{k_1 \rho_p / D_e}$, and, therefore, of α, and not of Φ_s. The second term in the denominator of Eq. (11-104), which is positive, tends to reduce F. When this term is negligible, $F = 1 - \alpha$. This is represented by curve A in Fig. 11-14. For these conditions of $\eta \to 1$, Φ_s will be of the order of 1.0 and $\Phi_c = \frac{1}{3}$. Then the second term in the denominator is small and F is not much less than that given by curve A. Curve C in the figure corresponds to these conditions.

For the opposite situation of a very fast main reaction ($\Phi_c > 5$), the effectiveness factor is given by an expression similar to Eq. (11-54). However, it is written for the active core, so that

$$\eta = \frac{1}{\Phi_c} = \frac{r_s}{r_c}\frac{1}{\Phi_s} = \frac{1}{(1-\alpha)^{1/3}}\frac{1}{\Phi_s} \tag{11-105}$$

Then Eq. (11-104) becomes

$$F = \frac{1}{1\,(1-\alpha) + 3\Phi_s[1-(1-\alpha)^{1/3}]\,(1-\alpha)^{2/3}} \tag{11-106}$$

For $\Phi_s \geq 5$, Φ_s will be even larger. For $r_c/r_s = \frac{1}{3}$, $\Phi_s \geq 15$. Curve *D* in Fig. 11-14 is a plot of Eq. (11-106) with $\Phi_s = 15$. In this case a sharp drop in activity is observed. Physically, the situation corresponds to a large diffusion resistance or a fast main reaction. The reactant molecules cannot penetrate far into the active part of the catalyst before reaction occurs. Thus both the poisoning and main reaction compete for sites on the same (outer) surface. As the outer surface is poisoned, the rate falls dramatically.

Our discussion has expressed the effect of poisoning (F) in terms of the fraction, α, of the catalytic surface that has been poisoned. Perhaps a more important practical problem is how F varies with time. To obtain this information the relation between α and time is required. For *pore-mouth* poisoning this means finding the relation between (r_c/r_s) and t for the shell model. Such problems are identical to those considered in Chap. 14 for gas-solid noncatalytic reactions where a product of the reaction is also a solid. Quantitative relationships between (r_c/r_s) and t, based upon the shell model, are developed in Sec. 14-3. For *uniform distribution of poison*, the relation between α and time does not involve intraparticle diffusion for the poisoning reaction but only its intrinsic kinetics. A simple example of the type of equation to be solved is

$$\frac{dn}{dt} = k_p C_p (1-\alpha) \tag{11-107}$$

where n and C_p are the adsorbed and fluid phase concentrations of the poison. In this expression it is assumed that the rate of deposition of the poison is first order in C_p and in the fraction, $1-\alpha$, of unpoisoned surface. If monomolecular adsorption is assumed, n is proportional to α; that is $\alpha = n/n_0$, where n_0 is the adsorbed concentration corresponding to complete deactivation (a monomolecular layer of deposited poison). Then Eq. (11-107) can be written

$$\frac{d\alpha}{dt} = (k_p/n_0)C_p(1-\alpha) \tag{11-108}$$

Integration of this expression gives the required relationship between α and t. It may be combined with curves *A* or *B* in Fig. 11-14 to determine how F varies with time (see Prob. 11-16).

We should again mention that this discussion has been limited to *parallel and independent poisoning*, caused, for example, by deposition of an impurity in the reaction stream. For *series fouling* the equations relating F and α, and α and t are coupled. They become partial differential equations and their simultaneous solution becomes more complex† when intraparticle diffusion is involved (see Prob. 11-17 for a special, simple case).

† For a more complete analysis of the effects of both parallel and series poisoning see Shinobu Masamune and J. M. Smith, *AIChE J.*, **12**, 384 (1966).

PROBLEMS

11-1 In a cylindrical pore of 30 Å radius at what pressure would the bulk diffusivity in a $H_2-C_2H_6$ mixture be equal to the Knudsen diffusivity for H_2? The temperature is 100°C.

11-2 At 10 atm pressure and 100°C what would be the pore radius for which bulk and Knudsen diffusivities would be equal for H_2 in the hydrogen-ethane system. Locate a curve for equal values of bulk and Knudsen diffusivities on coordinates of pressure-vs.-pore radius. Mark the regions on the figure where Knudsen and where bulk diffusivity would be dominant.

11-3 Constant-pressure diffusion experiments are carried out in the apparatus shown in Fig. 11-1 with the H_2-N_2 binary system. In one experiment the nitrogen diffusion rate through the porous pellet was 0.49×10^{-5} g mol/s. What would be the counterdiffusion rate of hydrogen?

11-4 Diffusion rates for the H_2-N_2 system were measured by Rao and Smith† for a cylindrical Vycor (porous-glass) pellet 0.25 in. long and 0.56 in. in diameter, at 25°C and 1 atm pressure. A constant-pressure apparatus such as that shown in Fig. 11-1 was used. The Vycor has a mean pore radius of 45 Å, so that diffusion was by the Knudsen mechanism. The diffusion rates were small with respect to the flow rates of the pure gases on either side of the pellet. The average diffusion rate of hydrogen for a number of runs was 0.44 cm³/min (25°C, 1 atm). The porosity of the Vycor was 0.304.

(*a*) Calculate the effective diffusivity D_e of hydrogen in the pellet. (*b*) Calculate the tortuosity using the parallel-pore model. (*c*) Predict what the counterdiffusion rate of nitrogen would be.

11-5 Figure 11-2 displays a dynamic method for measuring the effective diffusivity in a catalyst pellet. Equation (11-21) relates D_e to the first moment μ_1 of the response peak measured at the detector. This expression is applicable when the volumetric flow rate Q_L in the chamber on the lower side of the pellet (Fig. 11-2) is very large.

(*a*) Derive a relationship between D_e, μ_1, pellet length (Δr), pellet porosity ε_p, and Q_L when Q_L is *not* especially large.

(*b*) Show that the equation obtained in (*a*) reduces the Eq. (11-21) when $Q_L \to \infty$.

Notes:

1. Neglect the accumulation of diffusing component in the small volume of the lower chamber.
2. Assume that turbulence in the lower chamber is such that there is negligible mass-transfer resistance between the bottom face of the catalyst pellet and the gas in the lower chamber.
3. Assume that the composition of gas throughout the lower chamber is uniform at any instant.

11-6 Rao and Smith†† also studied the first-order (at constant total pressure) reversible reaction

$$o\text{-}H_2 \rightleftharpoons p\text{-}H_2$$

at −196°C and 1 atm pressure using a NiO-on-Vycor catalyst. For particles with an average diameter of 58 microns, rate measurements gave $\mathbf{r}_p/(y_s - y_{se})_{o-H_2} = 5.29 \times 10^{-5}$ g mol/(s)(g catalyst). For *pellets* ⅛-in. long and ½-in. in diameter $\mathbf{r}_p/(y_s - y_{se})_{o-H_2} = 2.18 \times 10^{-5}$. The catalyst pellets were encased on the cylindrical surface and on one end, so that hydrogen was available only to the other face of the cylinder, as illustrated in Fig. 11-10. The density of the pellet was 1.46 g/cm³.

(*a*) From the experimental rate data evaluate the effectiveness factor for the pellet. (*b*) Using the random-pore model to estimate D_e, predict an effectiveness factor for comparison with the answer to part (*a*). Only micropores ($\bar{a}_p = 45$ Å) exist in Vycor, and the porosity of the pellet was $\varepsilon_p = 0.304$.

11-7 Cunningham et al.‡ measured global rates of ethylene hydrogenation on copper-magnesium oxide catalysts of two types: particles of 100 mesh size and ½-in. spherical pellets of three pellet densities. For both materials external concentration and temperature differences were negligible. The

† M. R. Rao and J. M. Smith, *AIChE J.*, **10**, 293 (1964).
†† Loc. cit.
‡ R. A. Cunningham, J. J. Carberry, and J. M. Smith, *AIChE J.*, **11**, 636 (1965).

rate data at about the same surface concentrations of ethylene and hydrogen at the outer surface of the particles and pellets are as shown below.

	Rate r, g mol (s)(g catalyst)			
		Pellets		
t_s, °C	Particles	$\rho_p = 0.72$	$\rho_p = 0.95$	$\rho_p = 1.18$
124	1.45×10^{-5}	6.8×10^{-6}	4.3×10^{-6}	2.2×10^{-6}
112	6.8×10^{-6}	6.7×10^{-6}	4.2×10^{-6}	2.1×10^{-6}
97	2.9×10^{-6}	6.4×10^{-6}	4.0×10^{-6}	2.0×10^{-6}
84	1.2×10^{-6}	6.0×10^{-6}	3.7×10^{-6}	1.9×10^{-6}
72	.....	5.5×10^{-6}	3.4×10^{-6}	1.7×10^{-6}
50	.....	4.3×10^{-6}	2.6×10^{-6}	1.3×10^{-6}

(*a*) From Arrhenius plots of these data, what is the true activation energy of the chemical steps at the catalytic sites? (*b*) Calculate effectiveness factors for pellets of each density at all the listed temperatures. (*c*) Explain why some effectiveness factors are greater than unity and why some are less than unity. (*d*) Why do the rate and the effectiveness factor increase with decreasing pellet density? (*e*) Suggest reasons for the very low apparent activation energies suggested by the pellet data. Note that even for the maximum effect of intrapellet gradients the apparent activation energy would still be one-half the true value.

11-8 Wheeler† has summarized the work on internal diffusion for catalytic cracking of gas-oil. At 500°C the rate data for fixed-bed operation, with relatively large ($\frac{1}{2}$-in.) catalyst particles and that for fluidized-bed reactors (very small particle size) are about the same. This suggests that the effectiveness factor for the large particles is high. Confirm this by estimating η for the $\frac{1}{2}$-in. catalyst if the mean pore radius is 30 Å, the particle diameter (spherical) is 0.31 cm, and the pore volume is 0.35 cm^3 g catalyst. Molecular weight of oil is 120.

At atmospheric pressure with 30-Å pores the diffusion will be of the Knudsen type. The rate data, interpreted in terms of a first-order rate equation, indicate (at atmospheric pressure) that $(k_1)_{exp} = 0.25$ cm^3/(s)(g catalyst). Assume that a tortuosity factor of 3.0 is applicable.

11-9 Blue et al.‡ have studied the dehydrogenation of butane at atmospheric pressure, using a chromia-alumina catalyst at 530°C. For a spherical catalyst size of $d_p = 0.32$ cm the experimental data suggest a first-order rate constant of about 0.94 cm^3/(s)(g catalyst). The pore radius is given as 110 Å. Assuming Knudsen diffusivity at this low pressure and estimating the pore volume as 0.35 cm^3/g, predict an effectiveness factor for the catalyst. Use the parallel-pore model with a tortuosity factor of 3.0.

11-10 Rate data for the pyrolysis of normal octane (C_8H_{18}) at 450°C give an apparent, first-order, irreversible rate constant, k_a, of 0.25 cm^3/(s)(g). This apparent rate constant is defined:

$$\text{r (mol/(s)(g catalyst)} = kC$$

where C_s = concn of hydrocarbon gas at outer surface of catalyst pellet, mol/cm^3.

The data were obtained at 1 atm pressure with a monodisperse, silica catalyst whose average pore size was 30 Å. At these conditions Knudsen diffusion predominates in the pores. Other properties of the $\frac{1}{8}$-in., spherical catalyst pellets are as follows: surface area = 230 (m^2)/(g catalyst), pore volume = 0.35 cm^3/g, and tortuosity factor = 2.0. Using the parallel pore model, determine the effectiveness factor for this reaction-catalyst system.

† A. Wheeler in W. G. Frankenburg, V. I. Komarewsky, and E. K. Rideal (eds.), "Advances in Catalysis," vol. III, pp. 250–326, Academic Press, Inc., New York, 1950.

‡ R. W. Blue, V. C. F. Holm, R. B. Reiger, E. Fast, and L. Heckelsberg, *Ind. Eng. Chem.*, **44**, 2710 (1952).

11-11 In Example 11-8 effectiveness factors were calculated from global rate data for the liquid-phase hydrogenation of α-methyl styrene. The dissolved hydrogen concentration was constant in the differential reactor. The global rate was calculated from the cumene concentration C_c in the effluent liquid, the volumetric liquid flow rate Q, and the mass m of catalyst, by the conventional equation

$$r = \frac{QC_c}{m}$$

Explain, with appropriate equations, how the solution would need to be modified if C_{H_2} in the liquid varied from entrance to exit of the reactor.

11-12 (*a*) Develop an expression for the effectiveness factor for a straight cylindrical pore of length $2L$. Both ends of the pore are open to reactant gas of concentration $C = C_s$. A first-order irreversible reaction $A \rightarrow B$ occurs on the pore walls. Express the result as $\eta = f(\Phi_p)$, where Φ_p is the Thiele modulus for a single pore. Take the rate constant for the reaction as k_s, expressed as mol/(cm^2)(s) × (g mol/cm^3). The pore radius is a and the diffusivity of A in the pore is D.

(*b*) How does the relationship $\eta = f(\Phi_p)$ compare with Eq. (11-55)? What is the relationship between Φ_p and Φ_L?

(*c*) Comparison of the definitions of Φ_p [derived in part (*a*)] and Φ_L [from Eq. (11-56)] leads to what relationship between the effective diffusivity D_e in a flat plate of catalyst and the diffusivity D for a single pore? Note that L, the actual thickness of the slab in Eq. (11-56), is equal to one-half the pore length. Also note that k_1 in Eq. (11-56) is equal to $k_s S_g$.

(*d*) What simple model of a porous catalyst will explain the relation between D_e and D? Assume that the Wheeler equation relating the pore radius, the pore volume, and the surface area [Eq. (11-23)] is applicable.

11-13 Consider the effect of surface diffusion on the effectiveness factor for a first-order, irreversible, gaseous reaction on a porous catalyst. Assume that the intrinsic rates of adsorption and desorption of reactant on the surface are rapid with respect to the rate of surface diffusion. Hence equilibrium is established between reactant in the gas in the pore and reactant adsorbed on the surface. Assume further that the equilibrium expression for the concentration is a linear one. Derive an equation for the effectiveness factor for each of the following two cases:

(*a*) A porous slab of catalyst (thickness L) in which diffusion is in one direction only, perpendicular to the face of the slab
(*b*) A spherical catalyst pellet of radius r.

Use the expression for total effective diffusivity given by Eq. (11-37) and follow the development in Sec. 11-7.

11-14 A limiting case of intrapellet transport resistances is that of the *thermal effectiveness factor*.† In this situation of zero mass-transfer resistance, the resistance to intrapellet heat transfer alone establishes the effectiveness of the pellet. Assume that the temperature effect on the rate can be represented by the Arrhenius function, so that the rate at any location is given by

$$r = Ae^{-E/R_gT} f(C_s)$$

where $f(C_s)$ represents the concentration dependency of the rate, evaluated at the outer surface of the pellet.

(*a*) Derive a dimensionless form of the differential equation for the temperature profile within the pellet, using the variables

$$T^* = \frac{T}{T_s} \qquad r^* = \frac{r}{r_s}$$

† J. A. Maymo, R. E. Cunningham, and J. M. Smith, *Ind. Eng. Chem., Fund. Quart.*, **5**, 280 (1966).

where T_s is the temperature at the outer surface of the pellet (radius r_s). What are the dimensionless coefficients in the equation? One of the parameters in the coefficient should be the rate of reaction evaluated at the outer surface; that is,

$$r_s = Ae^{-E/R_g T_s} f(C_s)$$

(*b*) Derive an integral equation for the effectiveness factor, where the integral is a function of the dimensionless temperature profile.

(*c*) Are the results in parts (*a*) and (*b*) restricted to a specific form for $f(C)$, such as a first-order reaction? (*d*) Would you expect the thermal effectiveness factor, given by the solution of the integral equation of part (*b*), to be more applicable to exothermic or to endothermic reactions? (*e*) Determine the effectiveness factor as a function of a dimensionless coefficient involving r_s, where the other coefficient is $E/R_g T_s = 20$.

A digital computer will facilitate the numerical solution of the equations derived in parts (*a*) and (*b*).

11-15 When the intrinsic rate of poison deposition on a porous catalyst is very fast with respect to intraparticle diffusion *pore-mouth* poisoning occurs. For these conditions a shell model (Fig. 11-15) can be used to approximate the effect of poisoning on the rate of a catalytic reaction. Equation (11-104) was presented to show the effect of the Thiele modules Φ_s for the main reaction and the effect of the size (x) of the poisoned shell on the rate. Show how Eq. (11-104) can be derived starting with the equations (11-98) and

$$r_p = m_p \eta k_1 C_c$$

11-16 The activity of a catalyst is known to decrease with time because of deposition of a poison in the feed stream. The poison-deposition reaction is intrinsically slow with respect to the rate of intraparticle diffusion of the poison. The rate of decrease of active catalyst surface is governed by Eq. (11-108). The main reaction is first order and irreversible. Also it is intrinsically fast so that intraparticle diffusion resistance is large. Derive an expression showing how the rate of the main reaction decreases with time for a constant poison concentration C_p.

11-17 As a simple illustration of series poisoning (for example, by carbon deposition in hydrocarbon cracking processes) consider the following reactions

$$A(g) \rightarrow B(g) \text{ main reaction } (B \text{ is desired product})$$

$$B(g) \rightarrow C(s) \text{ poisoning reaction (deposition of } C \text{ on catalyst)}$$

The main reaction is irreversible, first order in A, and its rate is directly proportional to the fraction of unpoisoned catalytic surface. The kinetics of the poisoning reaction obey Eq. (11-108) and its rate is slow with respect to the rate of intraparticle mass transfer.

(*a*) For a slow main reaction (no intraparticle diffusion) derive an equation showing how the rate of the main reaction decreases with time.

(*b*) Derive a similar expression for an intrinsically fast main reaction (large intraparticle diffusion resistance).

11-18 The "wetting efficiency" question in trickle-bed reactors introduces the problem of effectiveness factors in catalyst pellets with nonuniform boundary conditions. Consider a simple example of this problem for a catalyst pellet with slab geometry as sketched below. One face of the porous slab has a uniform concentration $C_{s,g}$ and the other face has a concentration $C_{s,\ell}$. Define the effectiveness factor η for a first-order reaction on the pore walls as:

$$\text{Rate [k mol (kg)(s)]} = \eta k C_{s,g}$$

k = first-order rate constant, m^3 (kg)(s)

ρ_p = density of porous catalyst slab, kg (m)$_3$

C = concentration of reactant in pores, k mol/(m)^3

A. Derive an expression for η in terms of the Thiele modules,

$$\Phi = L(k/\rho_p D_e)^{1/2}$$

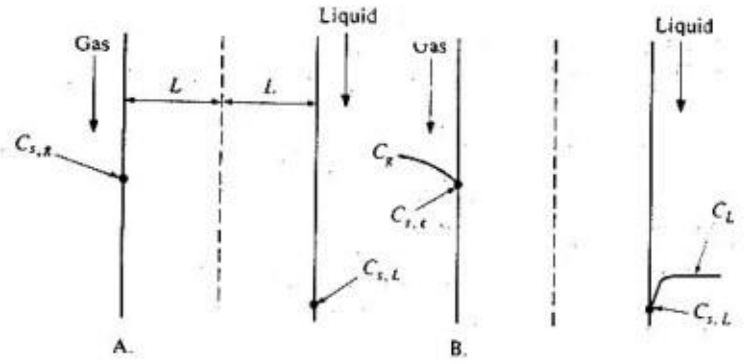

and the concentration ratio

$$C_{s,g}/C_{s,L}$$

where $2L$ = thickness of the slab, m

D_e = effective diffusivity of the reactant in the catalyst slab, m^2/s

B. How could external mass-transfer resistances on both faces of the slab be introduced in order to express the rate of reaction in terms of *bulk* concentrations C_g (see sketch) and C_L.